



Myoanatomy of three aberrant kinorhynch species: similar but different?

Maria Herranz^{1,2} · Katrine Worsaae¹ · Taeseo Park³ · Maikon Di Domenico⁴ · Brian S. Leander⁵ · Martin V. Sørensen²

Received: 5 December 2020 / Revised: 28 January 2021 / Accepted: 30 January 2021
© The Author(s), under exclusive licence to Springer-Verlag GmbH, DE part of Springer Nature 2021

Abstract

Aberrant kinorhynchs show several modifications deviating from the typical kinorhynch body plan, including a modified introvert with very elongated and flexible scalids, a weakly developed neck, and a slender trunk with less distinct segmentation. How these aberrant external features are reflected in the inner anatomy and how their aberrant body plan evolved are not understood. Here, we provide a comprehensive and comparative myoanatomical study of three putatively, distantly related worm-like species: *Cateria styx*, *Franciscideres kalenesos* and *Zelinkaderes yong*. Despite the weak external segmentation of the trunk, the studied species show a distinct segmental arrangement of the musculature. However, this arrangement is shifted posteriorly with respect to the external segmentation, because the extremely thin and flexible cuticle is lacking the apodeme-like cuticular thickenings (pachycycli) where the longitudinal muscles usually attach. The muscular arrangement in the three species is overall similar, yet, *C. styx* shows most resemblance to the allomalorhagid *F. kalenesos*, whereas the cyclorhagid *Z. yong* differs in several ways. This suggests a closer relationship of *C. styx* to Allomalorhagida. Whereas most kinorhynchs prefer muddy sediments, both the allomalorhagid and cyclorhagid worm-like kinorhynchs are mainly found in sandy environments, suggesting that a flexible, slender body evolved at least twice independently as an adaptation to the interstitial environment.

Keywords Mud dragons · Segmentation · Musculature · Meiofauna · CLSM · F-actin

Introduction

Kinorhynchs, commonly named mud dragons, have a quite conserved body plan with three well-differentiated regions: a head, a neck, and a segmented trunk. However, some genera with a characteristic worm-like appearance, exhibit significant modifications in one or more of these regions including: (i) introverts with reduced number of scalids; (ii) extremely

long and flexible primary spinoscalids; (iii) neck with poorly developed or lacking placids; (iv) slender trunk with very thin cuticle, and (v) less distinct external segmentation (Dal Zotto et al. 2013; Neuhaus and Kegel 2015; Herranz et al. 2019; Yamasaki 2019).

The increasing number of observations and availability of worm-like species have led to questions about the adaptive functionality and evolution of the aberrant body plan in Kinorhyncha. The first aberrant, worm-like kinorhynch species described was *C. styx* Gerlach 1956, collected intertidally from a sandy beach in Macaé, Brazil (Gerlach 1956). *C. styx* possesses several unusual and distinct characters including a very thin cuticle, a different arrangement of tergal and sternal plates in the trunk, neck without differentiated placids, introvert modifications, and a unique dorsal organ (Gerlach 1956; Herranz et al. 2019). The genus accommodates one additional species, *C. gerlachi* Higgins, 1968, that also lives intertidally and is described from a sandy beach in Waltair, India (Higgins 1968). Additional aberrant genera are: *Zelinkaderes* described by Higgins (1990), with five species from sandy and muddy sediments; *Triodontoderes* described

✉ Maria Herranz
maria.herranz@bio.ku.dk; mariaherranzm@gmail.com

¹ Department of Biology, University of Copenhagen, Copenhagen, Denmark

² Natural History Museum of Denmark, University of Copenhagen, Copenhagen, Denmark

³ National Institute of Biological Resources, Incheon, South Korea

⁴ Centro de Estudos Do Mar, Universidade Federal Do Paraná, Pontal do Paraná, Brazil

⁵ Departments of Zoology and Botany, University of British Columbia, Vancouver, Canada

by Sørensen and Rho (2009) with two species from coarse sediment, one from Micronesia (Sørensen and Rho 2009) and one from the Caribbean (Cepeda et al. 2019); and the monotypic genera *Franciscideres* described by Dal Zotto et al. (2013) and *Gracilideres* described by Yamasaki (2019) from coarse sediments in Brazil and in Japan, respectively.

The most recent phylogenetic analysis combining molecular and morphological data suggested *Franciscideres* and *Gracilideres* as sister groups nested within the Allomalorhagida (“new genus” in Sørensen et al. 2015); this result supported previous molecular analyses by Dal Zotto et al. (2013) and Yamasaki et al. (2013) where *Gracilideres* is referred to as “undescribed” or “new genus”, respectively. On the contrary, *Zelinkaderes*, *Triodontoderes* and *Cateria* were nested within Cyclorhagida (Sørensen et al. 2015). However, the lack of molecular data for *Cateria* makes its position within Cyclorhagida contentious because morphological similarities suggest a closer relationship with *Franciscideres* and *Gracilideres* (Sørensen et al. 2015; Yamasaki 2019).

Most studies on aberrant kinorhynchs have focused on their taxonomy, external morphology, phylogeny and ecology (Dal Zotto et al. 2013; Neuhaus and Kegel 2015; Sørensen et al. 2015; Herranz et al. 2019; Lopes Mello et al. 2019; Yamasaki 2019; Rucci et al. 2020), but little is known about their internal morphology. Only some aspects of *C. styx* and two other *Zelinkaderes* species (*Zelinkaderes brighiae* Sørensen et al. 2007 and *Z. floridensis* Higgins, 1990) have been studied using confocal laser scanning microscopy (CLSM) and transmission electron microscopy (TEM) (Neuhaus 1994; Herranz et al. 2013, 2019). Kinorhynchs with well-defined outer trunk segmentation also have correlating and segmentally arranged organ systems such as the musculature or the nervous system (Nebelsick 1993; Müller and Schmidt-Rhaesa 2003; Herranz et al. 2013, 2014, 2019, 2020; Altenburger 2016). However, it is still unclear how the internal morphology is organized in worm-like kinorhynchs with a thin cuticle and poorly differentiated trunk segments. With kinorhynchs being the only segmented taxon within the major ecdysozoan clade Cycloneuralia, investigations of the internal morphology of aberrant kinorhynchs are thus relevant to understand the evolution of segmentation, not only within Kinorhyncha but also within Ecdysozoa.

The aim of the present study is to investigate if the external morphology that characterises aberrant kinorhynchs is correlated with modifications in the arrangement of the internal organ systems. Here, we focus on the muscular system, using CLSM and F-actin staining to reconstruct three dimensionally the myoanatomy of three species and genera: *C. styx*, *F. kalenesos* Dal Zotto et al. 2013 and *Zelinkaderes yong* Altenburger et al. 2015. Through examination and comparison of distantly related representatives of both Allomalorhagida and Cyclorhagida, we establish hypotheses

on putative convergences and homologies in the musculature and anatomy of worm-like Kinorhyncha and their adaptations to the interstitial environment.

Materials and methods

Sampling

Specimens of *Z. yong* were collected in May 2018 intertidally from fine sand, at Geumneung Beach (33°23'23"N, 126°14'04"E) located at the northwest coast of Jeju Island, South Korea. Sediment samples were collected by hand. Specimens of *F. kalenesos* were collected in Mar 2015 and Jan 2019 from sandy beaches in Guaratuba, Brazil by the end of “Rua Bolivia”, and in Pontal do Paraná, Brazil “Praia das Gaivotas” (25°55'47"S, 48°34'48"W; 25°43'07"S, 48°28'49"W, respectively). Sediment samples were collected subtidally from the surf zone area by hand. Specimens of *C. styx* were collected in Mar 2015 at Cavaleiro Beach by the end of the street “Rua Bariloche” in Macaé, Brazil (22°21'59"S, 41°46'27"W). Sediment samples were collected from 50–70 cm deep holes dug on the beach, 3 m below the high tide mark. At all sampling localities, kinorhynchs were extracted from the sediment by stirring vigorously an equal mix of sediment and sea water in a bucket, letting the sediment deposit, and filtering the supernatant immediately after through a 60 µm mesh. The concentrated meiofauna was sorted while the specimens were still alive.

Histochemistry and confocal laser scanning microscopy (CLSM)

Specimens of *C. styx*, *F. kalenesos* and *Z. yong* were isolated from live samples, relaxed with a MgCl₂ solution for 5–10 min and fixed in 4% paraformaldehyde (PFA) in filtered sea water for 40–50 min at room temperature. Posteriorly, the specimens were washed at least three times in phosphate-buffered saline (PBS) and stored at 4 °C in PBS with 0.05% of sodium azide (NaN₃) to prevent microbial growth.

Myoanatomical studies were carried out with selected specimens of each species (25 *C. styx*, 16 *F. kalenesos* and 10 *Z. yong*). Specimens were first incubated in PBT (PBS 1x + 0.25% bovine serum albumin + 1% Triton X-100) for 30 min at room temperature. Posteriorly, the specimens were transferred to a mix of 0.33 M Alexa Fluor® either 488- or 633-labeled phalloidin (Invitrogen, Carlsbad, USA) in PBT and incubated at room temperature for 72 h in glass spot plates. Prior to mounting, the specimens were rinsed several times in 1 × PBS.

To guide interpretations of the myoanatomy of each species, imaging of the cuticle was carried out in combination

with the musculature. In Alexa Fluor® 633 stainings, the autofluorescence of the cuticle was acquired as a separate channel with an excitation wavelength of 488 nm. In specimens stained with Alexa Fluor® 488, the cuticle signal was captured together with the phalloidin signal.

For CLSM imaging, specimens were individually mounted on glass slides in Vectashield® antifade mounting medium containing DAPI (Vector Laboratories, Burlingame, USA). Specimens were imaged using an Olympus IX 8 inverted microscope in combination with a FluoView FV1000 confocal system at the Biological Institute, University of Copenhagen; and an Olympus FV1000 Multiphoton CLSM at the UBC Bioimaging Facility. Z-stacks were analysed and composed with FIJI, version 2.0 (Wayne Rasband, National Institutes of Health). Three-dimensional reconstructions were surface rendered from Z-stacks, segmented and labelled in Amira 6.0 (FEI, SAS). Original CLSM micrographs were edited (e.g., levels, rotation plane, contrast and brightness) with Adobe Photoshop CS6 (Adobe Systems Incorporated, San Jose, CA, USA) and Fiji. Figure plates were assembled in Adobe Illustrator CS6 (Adobe Systems Incorporated, San Jose, CA, USA).

Positional information used for the identification of external and internal anatomy, followed the commonly accepted terminology for kinorhynchs compiled in Sørensen and Pardos (2020).

Scanning electron microscopy (SEM)

Ten specimens of *F. kalenesos* fixed in 4% PFA were dehydrated through a water–ethanol series, and transferred to acetone through an ethanol–acetone series, critical point dried, mounted on aluminium stubs, sputter coated with a mix of platinum–palladium and examined under a JEOL JSM-6335F Field Emission SEM.

SEM specimens of *Z. yong* and *C. styx* from Altenburger et al. (2015) and Herranz et al. (2019) stored in MVS' collection were re-examined. Additional SEM photos of *Z. yong* were kindly provided by Andreas Altenburger.

Results

The three selected species *Z. yong*, *F. kalenesos* and *C. styx* are characterized externally by their vermiform appearance with very elongated trunk, circular in cross section, modified introvert and neck, extremely thin cuticle and less distinct trunk segmentation (Fig. 1). For detailed external descriptions of *Z. yong* see Altenburger et al. (2015); for *F. kalenesos* see Dal Zotto et al. (2013) and Rucci et al. (2020); for *C. styx*, see Higgins (1968), Neuhaus and Kegel (2015) and Herranz et al. (2019). Detailed data of all myoanatomical

studies on kinorhynchs to date, including the results presented herein, are compiled in Table 1.

Myoanatomy of *Z. yong*

Introvert

The introvert in *Z. yong* is supplied by several muscles including ten primary spinoscalid muscles, ten spinoscalid retractors, ten bundles of long retractors, three circular muscles and twelve short retractors. The primary spinoscalid muscles (psm) are intrinsic to each of the ten primary spinoscalids. They originate on the proximal part of the basal spinoscalid piece, and insert at the base of the distal end-piece; therefore, allowing independent movement of each primary spinoscalid (Fig. 2a, c, g). The primary spinoscalid muscles reach their maximum length when the introvert is retracted in the trunk and the spinoscalids are straight (Fig. 2a, g). The spinoscalid retractors (sr) are a V-shaped when the introvert is retracted (Fig. 2a), inserting alternate to the primary spinoscalids and originating at the introvert base. The introvert long retractors (ilr) are grouped into ten bundles of four muscles each, including two thick and two thin muscles. The ten bundles originate adjacent to the V-shaped spinoscalid retractors, and extend posteriorly to insert trunk segments 4–8 in laterodorsal/midlateral and ventromedial positions, respectively (Figs. 2a, c, g, 3a, b). The introvert circular muscles (icm) insert at the posteriormost part of the introvert cuticle (Fig. 2a, b). Their position varies depending of the degree of extension of the introvert, being posterior to the neck muscles when the introvert is retracted and anterior when the introvert is extended (Figs. 2a, b, 3f). The introvert short retractors (isr) are radially arranged. They originate anteriorly adjacent to the introvert circular muscles of the introvert, and insert posteriorly to the cuticle of segment 1 (Figs. 2a, b, f, 3).

Mouth cone and gut musculature

Musculature associated with the mouth cone and gut in *Z. yong* includes nine pairs of outer oral style longitudinal muscles, nine short basal oral style muscles, one circular muscle, inner oral style muscles, a pharyngeal bulb surrounded by pharynx-associated muscles, and intestine-associated muscles. A pair of outer oral style muscles (osm) is associated with each of the nine outer oral styles and situated along their most proximal part (Fig. 2a, g). The short basal outer oral style muscles (bosm) lay in between the bases of the outer oral styles, associated with soft cuticle (Fig. 2g). A circular muscle is present at the basal part of the outer oral styles, situated internally respect to the other muscles (osm, bosm) and is composed of three fibres. Additionally, associated with the base of the inner oral styles there are several

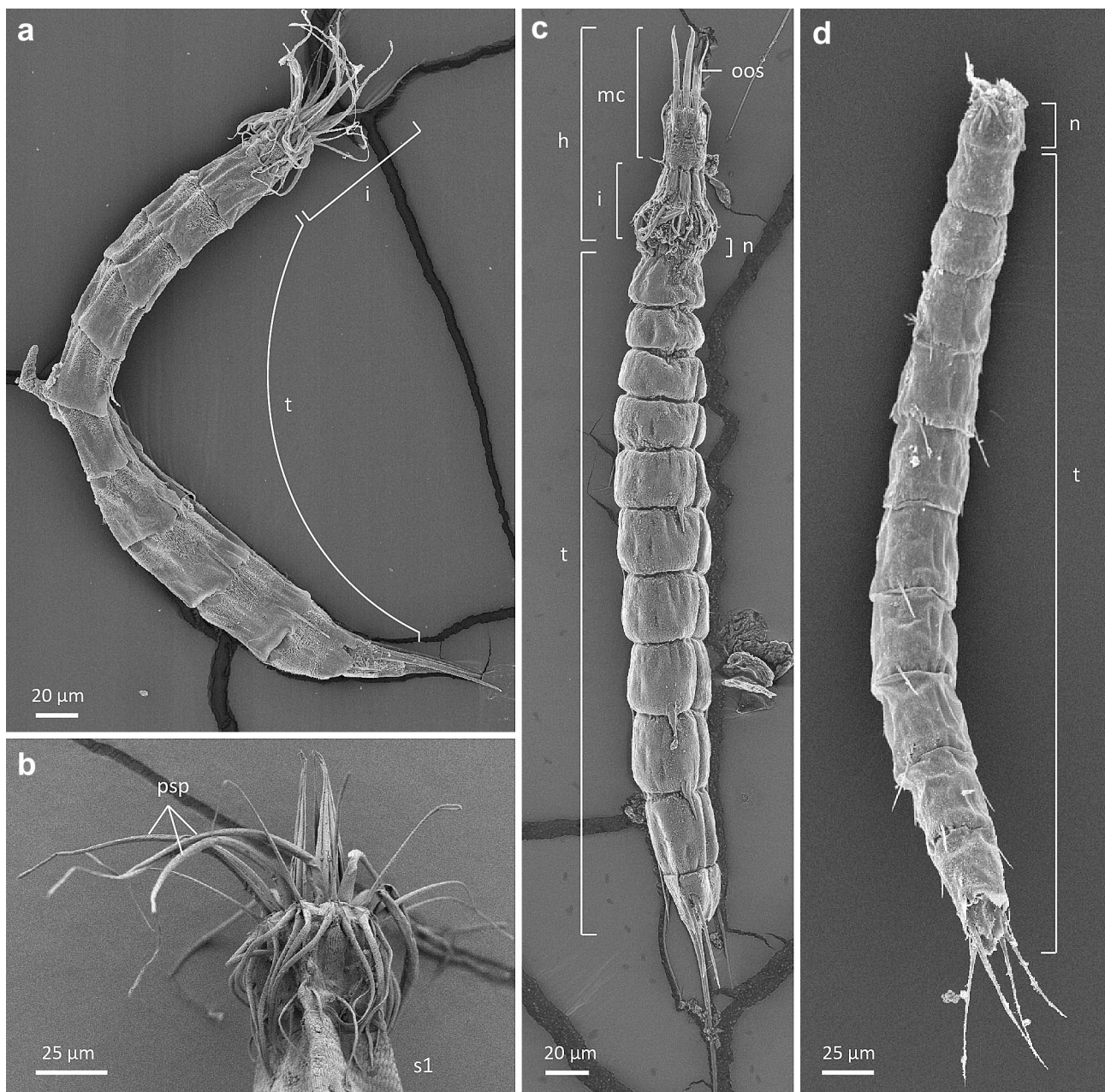


Fig. 1 External anatomy of *Cateria styx*, *Franciscideres kalenesos* and *Zelinkaderes yong*. Scanning electron micrographs. All views with anterior to the top and dorsal to the left. **a** Lateral view of *C. styx*, with the introvert everted, mouth cone retracted, dorsal organ extended. **b** Detail of *C. styx* introvert, notice the very elongated pri-

mary spinoscalids. **c** Lateral view of *Z. yong*, with the introvert and mouth cone fully extended. **d** Lateroventral view of *F. kalenesos*, head retracted. Abbreviations: *h* head, *i* introvert, *mc* mouth cone, *n* neck, *oos* outer oral styles, *psp* primary spinoscalids, *s1* segment 1, *t* trunk

short muscles arranged in a ring-like structure (iosm). The anterior part of the ring-like structure shows short muscle fibres extending towards the first inner oral styles ring (also referred at as ring -01). These muscles are arranged in pairs and form a triangular shape giving the appearance of a crown with five tips, where each of the tips correspond with the position of an inner oral style (Figs. 2g, 3a, b, g). The pharyngeal bulb (pb) is situated below the inner oral

styles and composed of approximately 15 alternating circular and radial muscles (Figs. 2a, g, 3a, b, g). The pharyngeal lumen is circular in cross section. Several muscles supply the pharynx externally: pharynx retractor muscles, pharynx longitudinal muscles and gut longitudinal muscles. Eight to ten pharynx retractors (pr) originate radially adjacent to the anteriormost part of the pharyngeal bulb, and extend to segments 3–5, where they insert centrally (Figs. 2g, 3a, b, g).

Table 1 Compendium of all the available myoanatomical data in kinorhynchs. Asterisks mark aberrant kinorhynchs

Species	Data source	Introvert	Mouth cone	Pharynx	Gut	Neck	Trunk	Spines	References
<i>Antygomonas</i> sp.	CLSM	16 outer retractors reaching S.8	16 longitudinal, 8 short basal and 2 circular muscles	Circular lumen, 14–15 circular fibers alternate with inhomogeneous structures, pre- and post-pharyngeal sphincters 10 protractors, Pharynx-associated muscles “sheath”	Muscular grid: Inner longitudinal + outer circular Hindgut: 1 dilator muscle	2 circular muscles: inner, outer	Longitudinal muscles: ventrolateral + dorsolateral Diagonal: 9 pairs Dorsoventral: S.1–11	MTS muscles	Müller and Schmidt-Rhaesa (2003)
<i>C. styx</i> *	CLSM	10 spinoscalid retractors, 10 bundles of long retractors reaching S.4–6, 14 short retractors, 6 circular muscles	2 circular muscles, + 6 mouth cone retractors	Circular lumen, + 25 alternating circular and radial muscles, associated longitudinal muscles	Muscular grid: Inner longitudinal + outer circular Hindgut: 6 dilator muscles	Absent	Longitudinal muscles: ventromedial/ventrolateral + subdorsal/lat-erodorsal Lateral: S.1–9 Dorsoventral: S.1–11	1 pair LTAS transverse muscles	This study
<i>Dracoderes abei</i>	CLSM	10 primary spinoscalid muscles, 10 W-shaped spinoscalid retractors, 10 long retractor bundles reaching S.3–8, 12 short retractors, 3 circular muscles	5 sets of longitudinal muscles, 2 circular muscles	Circular lumen, + 16 alternating circular and radial muscles, 10 pharynx protractors, + 10 pharynx retractors, 10 pharynx longitudinal muscles	Muscular grid: Inner longitudinal + outer circular Hindgut: 4 dilators, 1 transverse muscle (constrictor)	7 polygonal muscles	Longitudinal muscles: ventromedial/ventrolateral + subdorsal/lat-erodorsal + additional connective fibers Diagonal: S.2–5 Dorsoventral: S.2–11 Oblique muscles S.1 Tergal oblique muscles S.11	2 pairs LTS muscles, 2 pairs penile spine muscles in males	Herranz et al. (2020)
<i>Echinoderes aquilonius</i>	TEM	16 outer retractors, 12 inner retractor	–	Circular lumen, 1 postpharyngeal sphincter	12–16 longitudinal muscles	Circular muscle	–	–	Kristensen and Higgins (1991)

Table 1 (continued)

Species	Data source	Introvert	Mouth cone	Pharynx	Gut	Neck	Trunk	Spines	References
<i>Echinoderes capitatus</i>	TEM	10 outer retractors reaching S.6, 1 circular muscle	3 circular muscles	-	-	-	-	-	Nebelsick (1993)
<i>Echinoderes</i> sp. <i>E. dujardini</i> <i>E. hispanicus</i> <i>E. horni</i> <i>E. spinifurca</i>	CLSM	10 spinoscalid retractors, 10 long retractors reaching S.6, 14–16 short retractors, 1 circular muscle	18 longitudinal muscles, 10 radial + 10 circular 2 circular muscles	Circular lumen, 10 radial + 10 circular fibers, ca. 18 retractors, 10 inner and 4–6 outer protractors, 10 pharynx longitudinal muscles	Muscular grid: + 16 Inner longitudinal + 16 outer circular Hindgut: 2–4 short dilator muscles	1 circular muscle	Longitudinal muscles: Ventromedial + laterodorsal and additional con-tinuous fibers, Diagonal: S.1–8 Dorsoventral: S.3–10	2 pairs LTS muscles, 1 pair TE muscles, 1 pair penile spine muscles	Herranz et al. (2014)
<i>F. kalenesos</i> *	CLSM	10 spinoscalid retractors, 10 bundles of long retractors reaching S.3–6, 14 short retractors, 4–5 circular muscles	2 circular muscles, mouth cone retractors	Circular lumen, + 22 alternating circular and radial muscles, associated longitudinal muscles	Muscular grid: Inner longitudinal + outer circular Hindgut: 2 short dilator muscles, 1 constrictor muscle	1 circular muscle, longitudinal dorsal, ventral and lateral muscles	Longitudinal muscles: Ventromedial/ventrolateral + subdorsal Lateral longitudinal: S.1–9 Dorsoventral: S.1–11 Transverse muscle S.11	1 pair LTAS muscles	This study
<i>Pycnophyes iyocryptus</i>	CLSM	10 spinoscalid retractors, 10 short spinoscalid muscles, 10 sets of long retractors reaching S.3–6, 14 short retractors, 5 circular muscles	2 circular muscles, zig-zag muscles at the base of the mouth cone	Triradiate lumen, ca. 20 alternating circular and radial muscles, + 4 pharynx protractors, + 10 pharynx retractors, 10 pharynx-associated longitudinal muscles	Muscular grid: 16 inner longitudinal + outer circular Hindgut: hindgut sphincter	Placid longitudinal retractors, 2 transverse muscles, 4 neck retractors	Longitudinal muscles: ventromedial + subdorsal + additional continuous fibers Dorsoventral: S.1–10 Oblique muscle S.1	1 pair penile spine muscles, 1 pair of gonopore muscles	Herranz et al. (2020)

Table 1 (continued)

Species	Data source	Introvert	Mouth cone	Pharynx	Gut	Neck	Trunk	Spines	References
<i>Setaphyes dentatus</i>	TEM	10 head retractors	2 circular muscle cells basal to oos, 7 circular muscle cells basal to ios	Triradiate lumen, 13 radial + 14 circular alternating muscles, 1 postpharyngeal sphincter	Muscular grid: Inner longitudinal + outer circular Hindgut dilators: 2 caudal + 2 frontal + 3 transverse muscles	–	–	–	Neuhaus (1994)
<i>S. kielenensis</i>	TEM, CLSM	8 y-shaped muscles, 10 head retractors	2 circular muscles	Triradiate lumen, 13 radial + 14 circular alternating muscles, 1 postpharyngeal sphincter, 2 protractors, undetermined retractors, 9 mouth cone muscles	Muscular grid: Inner longitudinal + outer circular Hindgut dilators: 2 caudal + 2 frontal + 3 transverse muscles	Placid longitudinal retractors, 1 transverse muscle	Longitudinal muscles: Ventral and dorsal + additional continuous fibers Dorsoventral: S.1–11 Lateral longitudinal muscles S. 1–2	1 pair LTS muscles, 1 pair penile spine muscles	Altenburger (2016), Neuhaus (1994)
<i>Z. floridensis</i>	TEM	–	18 longitudinal oos muscles, 2 circular muscles	Circular lumen, 15 alternating circular and radial muscles, 2 prepharyngeal 1 postpharyngeal sphincters	Muscular grid: Inner longitudinal + outer circular Hindgut: 6 dilators: 2 caudal, 2 dorsal, 1 frontal, 1 circular	–	–	–	Neuhaus (1994)
<i>Z. yong*</i>	CLSM	10 primary spinoscalid muscles, 10 spinoscalid retractors, 10 bundles of long retractors reaching S.4–8, 12 short retractors, 3 circular muscles	18 longitudinal oos muscles, 9 short basal 1 circular muscle, ring-like inner oral style muscles	Circular lumen, 15 alternating circular and radial muscles, 8–10 retractors, 10 associated longitudinal muscles	Muscular grid: Inner longitudinal + outer circular Hindgut: 4 dilators, triangularly arranged constrictor muscles	3 thin circular muscles	Longitudinal muscles: Ventromedial/ventrolateral + subdorsal Lateral longitudinal: S.1–7 Dorsoventral: S.2–11	1 pair LTAS muscles, 1 pair MTS muscles	This study

LTAS lateral accessory spines, LTS lateral terminal spines, MTS midterminal spine, oos outer oral styles, – indicates absence of data

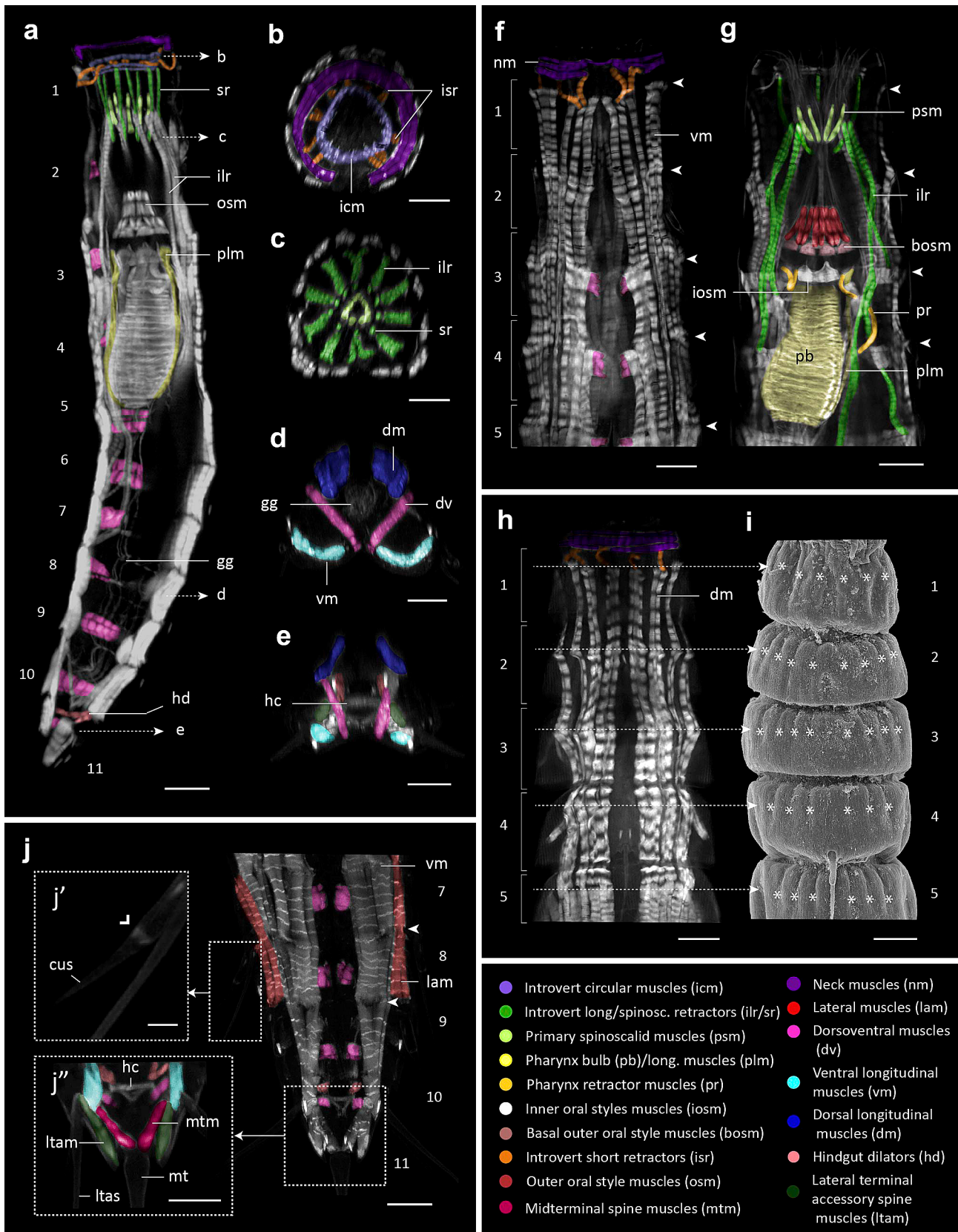


Fig. 2 Myoanatomy in *Zelinkaderes yong*. Z-stack projections of specimens labelled with phalloidin (**a–h, j**) and scanning electron micrograph of the cuticle showing marks of muscle attachments (**i**). Autofluorescence of the cuticle was kept for guidance in (**g, h, j**). Muscles of interest have been coloured in some panels according to the legend, which applies to all panels. Anterior is up in (**a, f–j**), dorsal is up in (**b–e**). **a** Lateral view showing a z-stack of the right side of the specimen. **b–e** Cross sections at different levels of the neck and trunk; levels of sections indicated by dashed lines and arrows in (**a**). **f, g** Neck and segments 1–5, head retracted, ventral view; (**f**) shows muscles associated with the trunk, (**g**) shows muscles associated with the introvert, mouth cone and pharynx. **h** Segments 1–5, dorsal view. Dashed lines mark the insertion points of longitudinal trunk muscles. **i** Cuticular details of segments 1–5, dorsal view. Asterisks mark the position of the muscle scars (seen as depressions) left by the muscle attachments in the cuticle. Note how the number of depressions fits with the number of longitudinal muscle bundles in (**h**). **j** Segments 7–11 ventral view. **j'** Detail of the dashed square marked on **j** showing phalloidin labelling in the cuspidate spines (arrowhead). **j''** Detail of segments 10–11 marked in (**j**) with a dashed square showing muscles associated with the terminal spines. Arrowheads mark attachment points of the longitudinal trunk muscles. Note that the segmental muscle attachment points are not coincident with the intersegmental areas. Numbers refer to segments. Scale bars: 20 μm (**a–c, f–h**), 10 μm (**d, e, i, j, j''**), 5 μm (**j'**). Additional abbreviations: *cus* cuspidate spine, *gg* gut grid, *hc* hindgut constrictor, *ltas* lateral terminal accessory spine, *mt* midterminal spine

When the pharynx is retracted into the trunk, these muscles get a wavy appearance (Figs. 2g, 3a, b). Ten pharynx longitudinal muscles (plm) originate from the posterior part of the pharyngeal bulb and insert at the posteriormost part of the mouth cone (Fig. 2a). Contraction of these muscles will shorten the pharyngeal bulb longitudinally. The gut longitudinal muscles (gl), surrounding the oesophagus and intestine, originate along the anterior third of the pharyngeal bulb and extend posteriorly towards segment 11. Multiple circular muscles encircle the longitudinal muscles of the gut forming a gut grid (gg) (Fig. 2a, d). The hindgut is associated with several muscles. Two pairs of muscles extend ventrally from their subdorsal origin in segment 10 and are interpreted as hindgut dilators (hd) (Figs. 2a, j, j'', 3a, b). The dorsoventral muscles in segment 11 also seem to supply the hindgut (Fig. 2e, j, j''). A set of muscles forming a triangular shape is situated medially in segment 11 surrounding the hindgut, interpreted to be hindgut constrictors (hc) (Figs. 2e, j, j'', 3a, b).

Neck

The neck region contains three thin circular muscles (nm). The two posterior muscles are consistently interrupted in paraventral position, whereas the anteriormost muscle is the only one forming a complete ring (Figs. 2b, f, 3).

Trunk

The trunk region in *Z. yong* is composed of several sets of muscles including dorsal, ventral, dorsoventral and lateral muscles. Some of the longitudinal muscles (dorsal, ventral and lateral) seem to expand across segments, whereas the dorsoventral muscles are segmentally arranged. The longitudinal muscles are arranged in separate sets, each of them composed of a single or several muscles. Eighteen longitudinal muscle sets originate at the anterior part of segment 1, where eight are dorsal, eight ventral and two lateral (Figs. 2f, h, 3). The only muscle sets composed of single muscles are situated in ventromedial positions (Figs. 2f, 3c, d, f). The dorsal, lateral and ventral longitudinal muscles originate in a transverse zone at the anterior 1/3 of the tegumental plates, extend across the intersegmental region, and insert in corresponding positions at the following segment. In this way, the segmental arrangement of the musculature is shifted 1/3 segment length in relation to the external, cuticular segment differentiation (Figs. 2f, h, 3c, d). The posterior insertion point of a longitudinal muscle is furthermore situated so close to the origin of the following muscle that it gives the illusion of several long and draped continuous muscles that extend through the entire trunk. The attachment points for these muscles form small muscular “scars” visible externally on the cuticular surface of each segment and detectable with SEM (seen as cuticular depressions in Fig. 2i). From segments 5–10, the dorsal and ventral longitudinal muscle sets become less distinguishable, forming two subdorsal and ventromedial groups, respectively (Fig. 3b). The lateral muscle bundles arise from midlateral to laterodorsal positions on segments 1–7 adjacent to the dorsal insertion of the dorsoventral muscles (Fig. 3d, e). However, it is not clear whether all the lateral muscles maintain a segmental arrangement in all the segments. Paired dorsoventral muscles are present from segments 2–11 and are composed of three fibres each, except for segments 2 and 3, where the muscles are shorter and limited to one or two fibres (Figs. 2a, f, j, 3). All the muscles have paraventral attachments but insert progressively more dorsal. On segments 2–3, the insertion points of the dorsoventral muscles are midlateral and reach a subdorsal position on segments 10–11 (Fig. 2d, e).

Additional muscles of the trunk supply the terminal spines. The midterminal spine is at its base supplied by a pair of diverging muscles (mtm) that insert in the anterior part of segment 11 (Figs. 2j, j'', 3a, b). A pair of muscles (ltam) supplies the lateral terminal accessory spines. These muscles originate at the base of the lateral terminal accessory spines and insert adjacent to the insertion of the midterminal spine (Fig. 2j, j''). Based on the position and arrangement of the muscles, we interpret that the midterminal and lateral terminal accessory spines can only move in the lateral

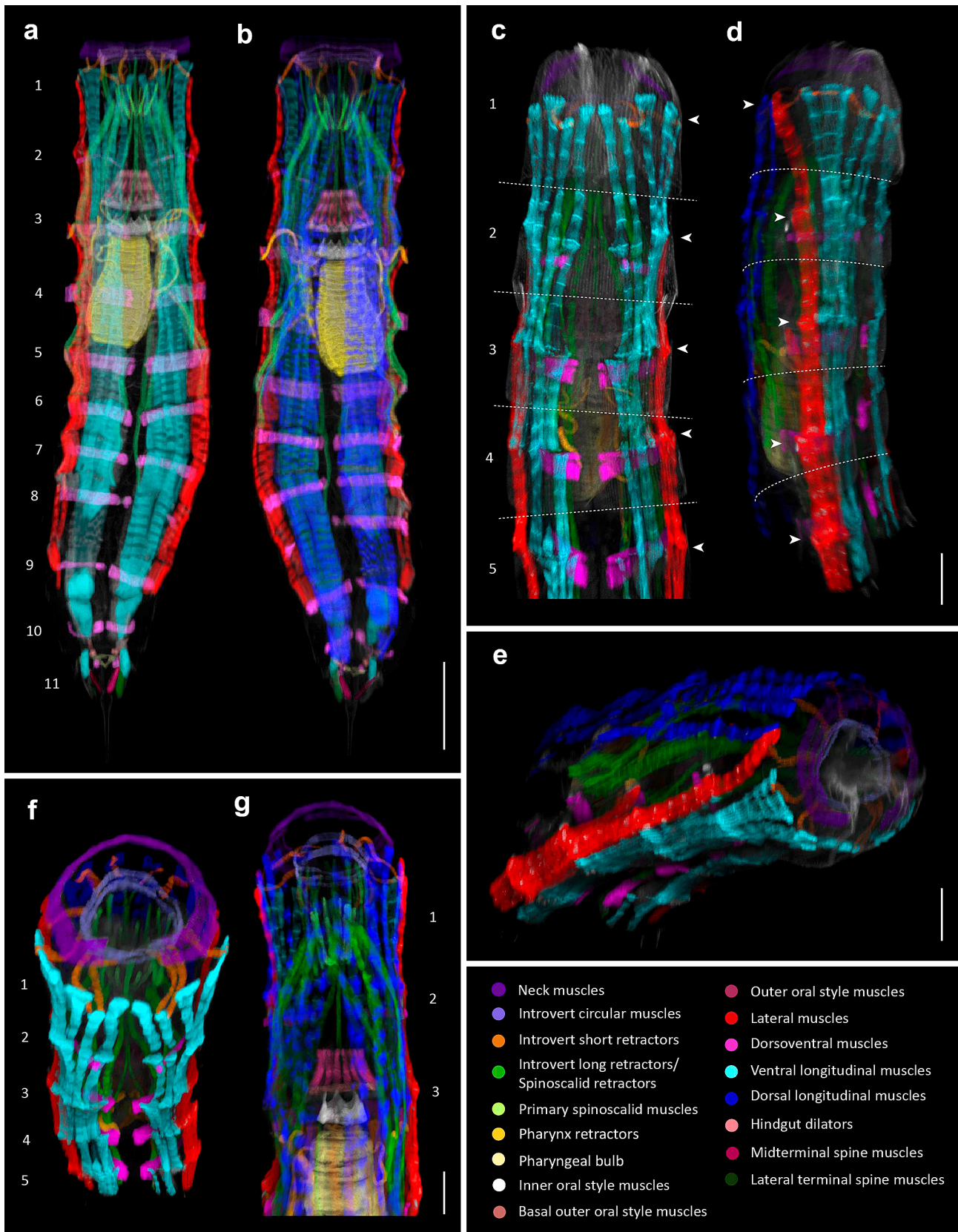


Fig. 3 Three-dimensional reconstruction of the myoanatomy in *Z. yong*. Autofluorescence of the cuticle was kept for guidance in (a–e). Anterior is up in (a–d, f, g), dorsal is up in (e). Colour legend applies to all panels. **a** Ventral overview. **b** Dorsal overview. **c, d** Segments 1–5, ventral and lateral views, respectively. Dashed lines mark segment limits, arrowheads mark the attachment points of longitudinal muscles. **e** Segments 1–5, apical–lateral view. **f** Segments 1–5 apical–ventral view. **g** Segments 1–3, dorsal view. Scale bars: 50 μm (a, b), 20 μm (c–g)

plane. Lateral terminal spines do not seem to be directly supplied by any muscles.

Moreover, weak F-actin labelling was found in the distal part of the cuspidate spines in the shape of a ring, indicating the presence of contractile tissue (Fig. 2j'). Non-muscular labelling shows paired cylinder-shaped structures congruent with the position of sensory spots.

Myoanatomy of *F. kalenesos*

Introvert

The introvert of *F. kalenesos* is supplied by ten spinoscalid retractors, ten bundles of long retractors, four to five circular muscles and fourteen short retractors. However, no muscles supply the primary spinoscalids. The spinoscalid retractor muscles (sr) are λ -shaped and originate at the introvert cuticle at the level of the second spinoscalid ring, alternating with the primary spinoscalids (Figs. 4a, 5a, b). When the introvert is inverted the spinoscalid retractor muscles become y-shaped (Figs. 4a, 5a). The introvert long retractor muscles (ilr) originate at the level of the second row of spinoscalids and extend posteriorly towards segments 3 or 5–6 inserting in midlateral/laterodorsal positions, adjacent to the dorsoventral muscles (Figs. 4a, 5b, e). On segment 4, the long retractor muscle attachments are displaced dorsally, adjacent to the laterodorsal longitudinal muscles (Figs. 4d, 5c). The introvert circular muscles (icm) are thin and their positions vary depending on the level of introvert eversion/retraction (Figs. 4a, b, d, 5a, b). When the introvert is everted, the most anterior introvert circular muscles are situated underneath the second spinoscalid ring and the most posterior ring is situated under the last spinoscalid ring (Fig. 5b). The introvert short retractor muscles (isr) originate anteriorly adjacent to the posteriormost circular muscle, and extend posteriorly towards segment 1 where they insert centrally (Figs. 4a, b, 5a, b). When the introvert is everted, these muscles reach their maximum length (Figs. 4a, 5b), and when the introvert is retracted they have a wavy appearance (Fig. 4b).

Mouth cone and gut musculature

The musculature associated with the mouth cone includes two circular muscles, a number of mouth cone retractors, a pharyngeal bulb, pharynx-associated muscles and intestine-associated muscles. All these structures are moveable and their positions change in an anterior–posterior direction. The mouth cone shows two circular muscles (mcc), one at the base of the outer oral styles and another at the base of the inner oral styles (Fig. 4c). Additionally, there are several mouth cone retractors that originate from laterodorsal and ventrolateral positions in segments 3–6 and extend inserting at the base of the mouth cone (Figs. 4c, 5e). The pharyngeal bulb (pb) is very elongated and composed of ca. 22 alternating radial and circular muscles (Fig. 4c); the lumen is circular in cross section. Pharynx longitudinal muscles and gut longitudinal muscles supply and surround the pharyngeal bulb. The pharynx longitudinal muscles (plm) originate at the base of the pharyngeal bulb and insert at the base of the mouth cone (Fig. 4c). The gut is surrounded by a net of longitudinal and circular muscles forming a gut grid (gg) (Fig. 4d). The gut longitudinal muscles (gl) originate adjacent to the pharyngeal bulb and extend towards the hindgut. In segment 10, associated with the hindgut, there is a circular-like muscle identified as a hindgut constrictor (hc). Additionally, a pair of dorsal muscles originates from the dorsal part of segment 10 and insert at the hindgut; these are interpreted as hindgut dilators (hd) (Fig. 4d, h).

Neck

The neck, which has the appearance and length of a segment, has a circular muscle (nm) situated in a central position (Figs. 4a, b, d, 5a, b). Longitudinal sets of dorsal, ventral and lateral muscles originate adjacent to the circular muscle leaving distinct oval muscular scars in the cuticle (Fig. 4e), and attach in the anterior part of segment 1 (Fig. 5a, c, d).

Trunk

Every trunk segment in *F. kalenesos* shows longitudinal (dorsal, ventral) and dorsoventral sets of muscles, except for segment 11 that lacks dorsal and ventral muscles. Most of the longitudinal muscles are segmentally arranged, although this segmentation is shifted approximately 1/3 of a segment length when compared with the external cuticular segmentation (Figs. 4g, 5c). Dorsal muscles are distributed in two bundles along the subdorsal position (Figs. 4d, g, 5c, d). Ventral muscles are more compacted forming bundles in ventromedial/ventrolateral areas. Additionally, lateral longitudinal muscles (lam) are present in segments 1–9 adjacent to the ventral longitudinal muscles in a ventrolateral/sublateral position (Figs. 4d, 5c, d). Dorsal, ventral and

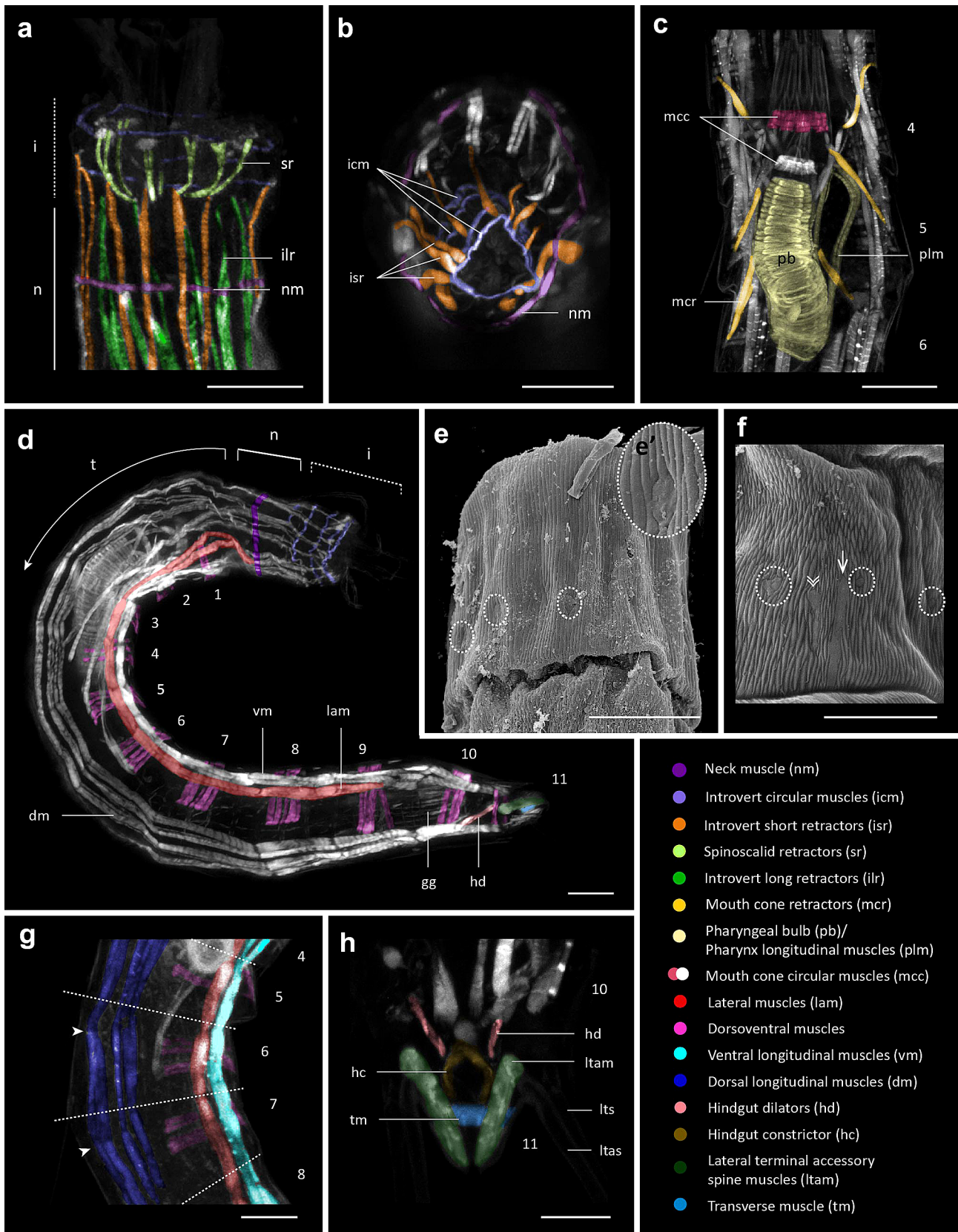


Fig. 4 Myoanatomy in *Franciscideres kalenesos*. Z-stack projections of specimens labelled with phalloidin (**a–d, g, h**), and scanning electron micrographs of the cuticle showing muscle attachment marks (**e, f**). Autofluorescence of the cuticle was kept for guidance in (**a, c, g, h**). Muscles of interest have been coloured in some panels according to the legend, which applies to all panels. Anterior is up in (**a, c, e–h**), dorsal is up in (**b, d**). **a** Detail of neck and partially open introvert, lateral view. **b** Apical view showing the neck, introvert withdrawn. **c** Muscles associated with the mouth cone and pharynx, lateral view. **d** Lateral overview, head partially everted. **e** Detail of the neck, dorsal view, (**e'**) close-up of muscular scar. **f** Detail of sternal plate, segment 3. Chevrons mark the muscular scar of a pharynx retractor; the arrow marks the elongated muscular scar from the dorsoventral muscle. Dashed circles mark muscular scars in (**e, f**). **g** Detail of trunk musculature on segments 5–7, lateral view. Dashed lines mark segment limits. Arrowheads mark the attachment points of the longitudinal muscles. Note that the segmental muscle attachments do not coincide with the intersegmental areas. **h** Detail of segments 10–11, dorsal view. Numbers refer to segments. Scale bars: 20 μm (**a–d, g**), 10 μm (**e, f, h**). Additional abbreviations: *gg* gut grid, *i* introvert, *lts* lateral terminal spine, *ltas* lateral terminal accessory spine, *n* neck, *t* trunk

lateral longitudinal muscles originate in the anteriormost part of one segment and extend towards the anterior third of the following segment where they insert leaving distinct round to oval muscular “scars” visible externally on the cuticle (Fig. 4f). The dorsoventral muscles (*dv*) are paired, segmentally arranged and composed of four to five fibres in most segments, except for segments 1 and 9–11 which have three or less fibres each (Figs. 4d, 5d). The dorsoventral muscles originate ventromedially and extend dorsally to insert midlaterally in segments 1–8 and laterodorsally in segments 9–11, leaving elongated muscular “scars” on the cuticle (Fig. 4f, marked with an arrow). Segment 11 has no dorsal or ventral sets of muscles but it shows at least a pair of strong longitudinal muscles associated with the lateral terminal accessory spines (*ltam*), interpreted as levator muscles. These muscles originate at the base of the lateral terminal accessory spines and insert to the posterior edge of the tergal plate, in the posterior part of segment 11 (Fig. 4h). The lateral terminal spines do not seem to be directly associated with any muscle; however, live observations show that both the lateral terminal and lateral terminal accessory spines are able to move posteriorly 90 degrees in a synchronized way during forward movement (Online resource 1). The closeness of the attachment points from the lateral terminal and lateral terminal accessory spines, and the evidence of synchronized movement, suggest that both spines could be connected internally by ligaments or cuticular processes. Additionally, segment 11 shows a short transverse muscle (*tm*), which function is undetermined (Fig. 4h). This muscle could be associated with the hindgut and, therefore, be interpreted as a hindgut dilator; or be involved in the movement of the lateral terminal accessory spines.

Non-muscular F-actin labelling appears as paired cylinder-shaped structures associated with the position of all sensory spots.

Myoanatomy of *C. styx*

Introvert

The introvert of *C. styx* is supplied by several sets of muscles including ten spinoscalids retractors, ten sets of long retractors, six thin circular muscles and ca. fourteen short retractors. The spinoscalid retractors (*sr*) are y-shaped when the introvert is retracted, they alternate in sizes between five short and five long muscles (Fig. 6b). Short and long spinoscalid retractors are distally associated with two different introvert circular muscles that are situated at the level of the second and third row of spinoscalids (Fig. 6b). The introvert long retractors (*ilr*) are grouped into ten bundles of three to four muscles each (Fig. 6b, d). These bundles originate anteriorly in the introvert cuticle, with their positions alternating with the ten spinoscalid retractors, and insert posteriorly to segments 4–6 in laterodorsal, midlateral and ventrolateral positions (Fig. 7a, d). The introvert circular muscles (*icm*) are distributed along the introvert and their positions change with the level of head eversion (Figs. 6b, 7b, c). Out of the six circular muscles, three supply different spinoscalid rows, one supplies the introvert short retractors, and the remaining two are located at the posteriormost part of the introvert, one below the trichoscalid level and another one at the anteriormost part of segment one. Based on their positions, the first three muscles are interpreted to be controlling the retraction of the spinoscalids together with the spinoscalid retractors. The fourth circular muscle is interpreted to reduce the diameter of the introvert, and the last two circular muscles work as closing apparatus in the absence of a well-differentiated neck. The introvert short retractors (*isr*) are radially arranged, and originate from the lower part of the introvert, at the level of the trichoscalids, adjacent to one of the introvert circular muscles (Figs. 6b, c, 7c). Posteriorly, they insert in the central part of the tegumental plate of segment 1. The introvert short retractors invert when the introvert is withdrawn (Fig. 6b).

Mouth cone and gut musculature

Musculature associated with the mouth cone and gut in *C. styx* includes two circular muscles, at least six mouth cone retractors, a pharyngeal bulb, pharynx-associated muscles and intestine-associated muscles. The two mouth cone circular muscles (*mcc*) are situated around the outer and inner oral styles (Fig. 6e). The outer oral style circular muscle is composed of four fibres while the inner oral style circular muscle has three fibres. The mouth cone retractors (*mcr*)

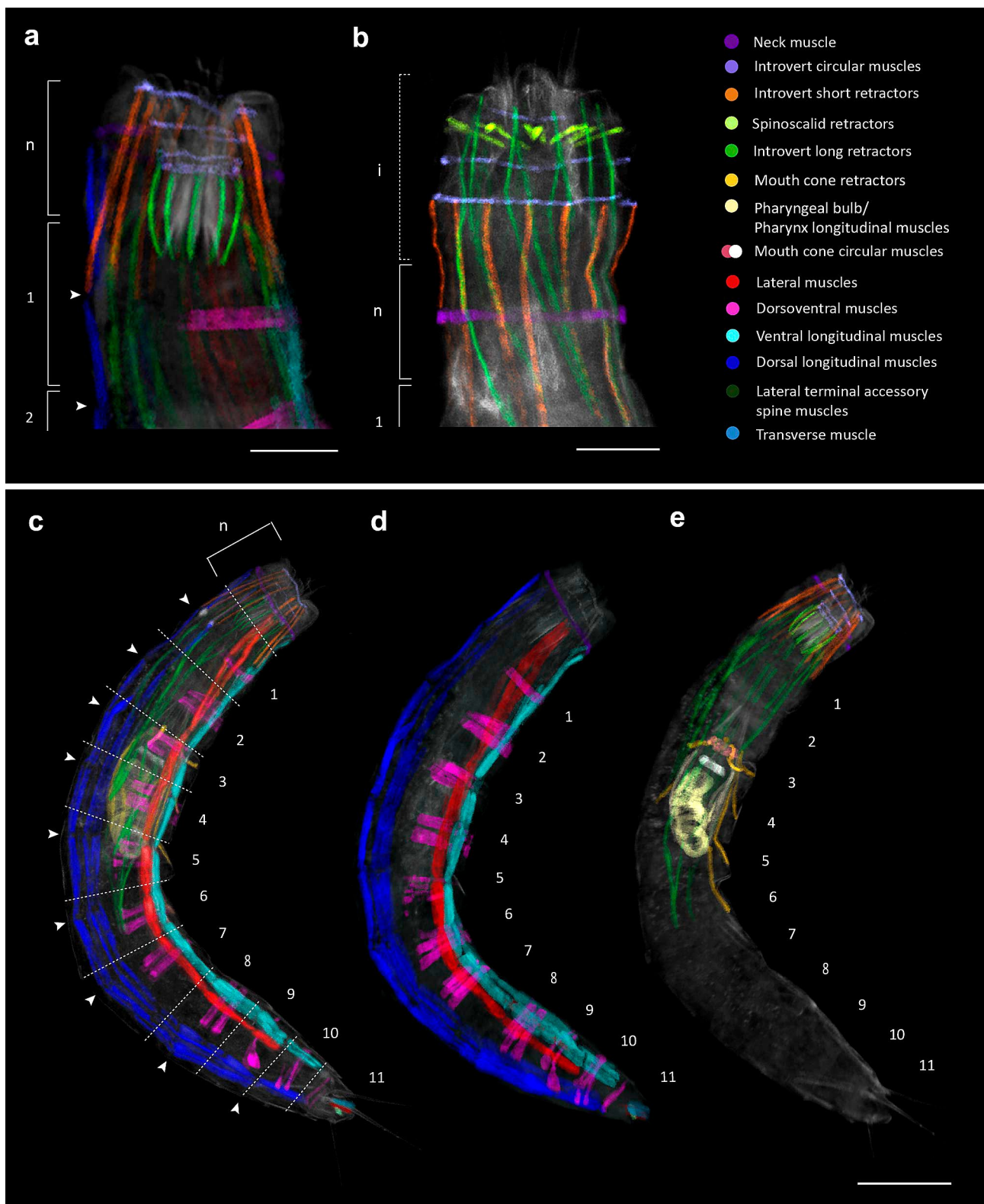


Fig. 5 Three-dimensional reconstruction of the myoanatomy in *Franciscideres kalenesos*. Autofluorescence of the cuticle was kept for guidance in all images, anterior is up and dorsal is to the left in all panels. Colour legend applies to all panels. **a** Detail of neck and segment 1, lateral view, head retracted. **b** Detail of partially everted introvert, neck and segment 1, lateral view. **c–e** Head and trunk asso-

ciated musculature, lateral view, head retracted. Arrowheads in **(a, c)** mark attachment points of the longitudinal muscles. Segments marked by brackets in **(a, b)**, dashed lines mark segment limits in **(c)**. Note that the muscle attachment points are not coincident with the intersegmental areas. Numbers refer to segments. Scale bars: 20 μm **(a, b)**, 50 μm **(c, d)**

originate adjacent to the anterior part of the pharyngeal bulb, at the base of the mouth cone and extend towards ventromedial and midlateral areas of segments 4–6 (Fig. 6e). The pharyngeal bulb is very elongated (ca. 80 μm in length), with more than 25 alternating circular and radial muscles and a lumen that appear circular in cross section. Pharynx-associated muscles include pharynx longitudinal muscles and gut longitudinal muscles. The pharynx longitudinal muscles (plm) originate at the posterior end of the pharyngeal bulb and extend anteriorly to insert to the basal part of the mouth cone (Fig. 6e). The gut longitudinal muscles originate adjacent to the pharyngeal bulb and extend posteriorly, surrounding the intestine. These muscles are encircled by circular muscles along the intestine forming a gut grid (gg) (Fig. 6h, j). The hindgut is associated with at least three pairs of short muscles. One pair originates from the dorsal part of segment 11, one from the ventromedial area, and one from midlateral position extending transversally towards the hindgut (Figs. 6h, j, 7a, b, e). These muscles are interpreted to be hindgut dilators (hd). A hindgut constrictor was not found; however, the action of the dorsoventral muscles of segment 11, closely associated with the hindgut (Figs. 6h, j, 7a, e), might have an antagonistic function to the dilator muscles, assisting the constriction of the hindgut.

Trunk

Every trunk segment in *C. styx* shows sets of longitudinal (dorsal, ventral) and dorsoventral muscles (Fig. 7a). These muscles are all segmentally arranged. The dorsal and ventral longitudinal segmental muscles originate in the anteriormost part of a segment and extend posteriorly inserting at the anteriormost part of the following segment (Fig. 7a), leaving distinct marks visible on the cuticle (chevrons Fig. 6g). The dorsal longitudinal muscles (dm) can be distinguished individually and extend along subdorsal and laterodorsal areas (Fig. 7d, e). The ventral longitudinal muscles are more compact and situate in ventromedial to ventrolateral areas (Fig. 7a, c). Additionally, strong lateral longitudinal muscles (lam) are present in segments 1–9 and seem to extend across segments (Figs. 6a, 7a, d, e). These muscles originate in a midlateral position in segments 1–6 and extend posteriorly in a diagonal way to insert in a ventrolateral/lateroventral position in segments 3–9 (Figs. 6a, 7a, d, e). Segments 10–11 are devoid of lateral muscles (Figs. 6a, h, 7a). The dorsoventral muscles are strong, composed of four to five fibres each, and insert centrally on the tegumental plate of each segment in midlateral and ventromedial positions leaving distinct elongated muscular scars (Fig. 6c, d, f, g, i). The dorsoventral muscles of segments 1 and 11 are smaller, with just three and two muscle fibres respectively (Fig. 6b, c, j). Segment 11 shows two pairs of short and strong longitudinal muscles overlapping each other. They

originate in the midlateral area, close to the bases of lateral terminal accessory spines, and extend in an oblique way towards the posterior part of segment 11, inserting midventrally (Figs. 6h, j, 7a, e). The function of these muscles is uncertain since they are not clearly connected with any of the terminal spines. A pair of short transverse muscles (tm) seems to supply the lateral accessory spines, originating at their bases and extending towards the centre of the segment to insert midventrally (Fig. 6h, j). The transverse muscles are interpreted as putative levator muscles. Lateral terminal spines without associated musculature. The midterminal spine does not seem to be directly connected with any muscles, and its movement is, therefore, interpreted as indirect, accompanying the movement of segment 11 (Fig. 6a, h). Live recordings of *C. styx* (Online resource 2) do not indicate any independent movement of the midterminal spine, which supports this interpretation.

Males of *C. styx* show a pair of funnel-shaped phalloidin labelled structures that extend longitudinally along segments 9–10 in a lateral position. The posterior end of each structure narrows and seems to connect in laterodorsal/midlateral position to segment 10 (Fig. 6i, arrows; 6j, dashed circle). The muscular nature of the described structures is uncertain but their position, close to the posteriormost part of the testis, and their absence in females, suggest it could be supplying the male reproductive system.

Discussion

Comparative myoanatomy in aberrant kinorhynchs

Despite sharing numerous general modifications that diverge from the typical kinorhynch anatomy, the aberrant species *Z. yong*, *F. kalenesos* and *C. styx* also show several differences in the organization of their underlying musculature.

Introvert and mouth cone

The introverts of the three studied species differ from the typical patterns by having extremely elongated primary spinoscalids and a reduced number of scalids with only 4–6 rows (Altenburger et al. 2015; Herranz et al. 2019; Rucci et al. 2020). However, there are also several differences regarding number and appearance of the spinoscalids among species (e.g., absence of trichoscalids in *F. kalenesos*, presence of hairy patches only in *C. styx* and *F. kalenesos*, or reduction of the second row of spinoscalids to fringes in *Z. yong*). Despite the observed differences, the musculature associated with the introvert is similar, and variation is restricted to the number of circular muscles and appearance of scalid-associated muscles. *Z. yong* has only three introvert circular muscles, whereas *F. kalenesos* shows four

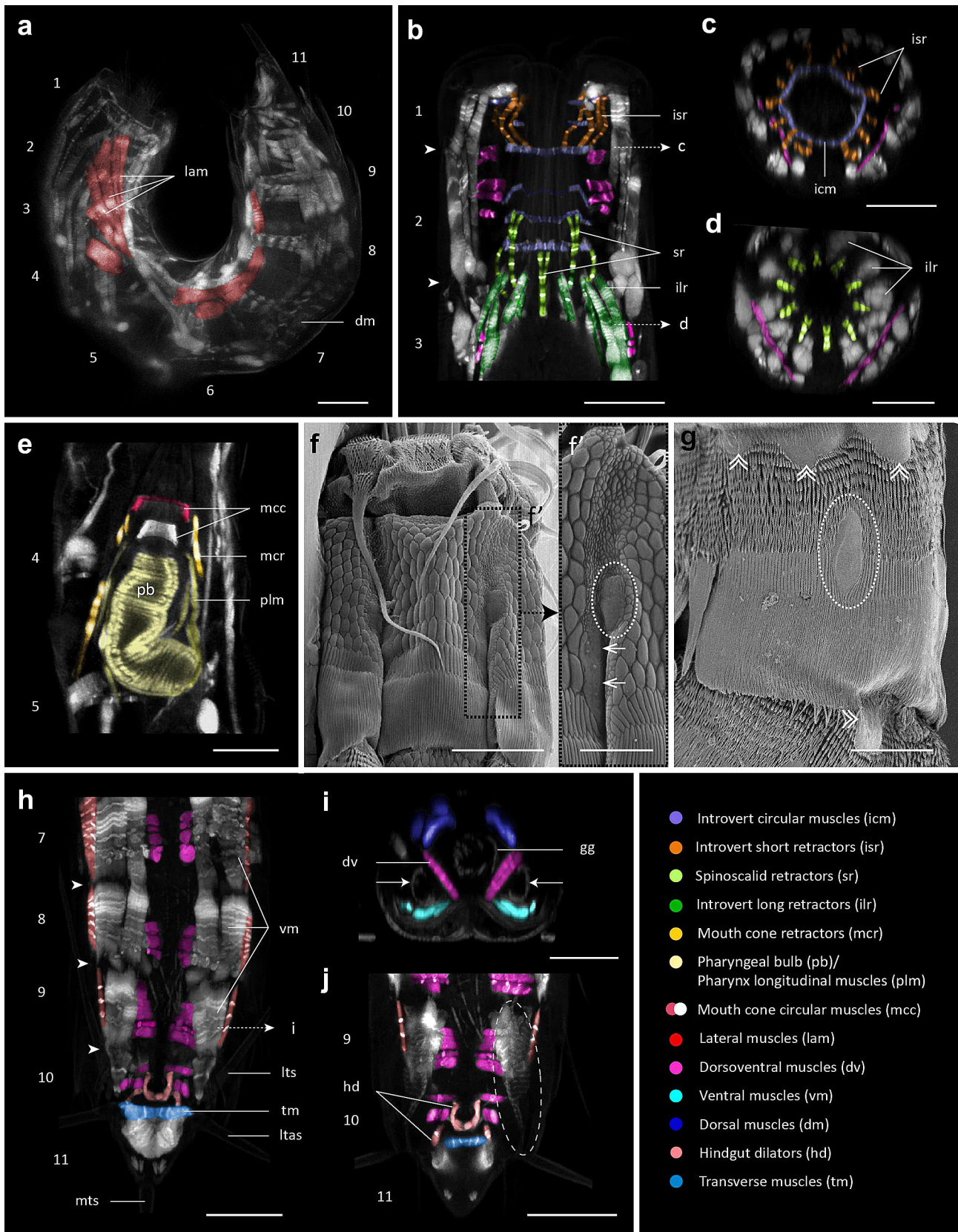


Fig. 6 Myoanatomy in *Cateria styx*. Z-stack projections of specimens labelled with phalloidin (**a–e**, **h–j**), and scanning electron micrographs of the cuticle showing muscle attachment marks (**f**, **g**). Autofluorescence of the cuticle was kept for guidance in (**a**, **b**, **e**, **h–j**). Muscles of interest have been coloured according to the legend, which applies to all panels. Anterior is up in (**a**, **b**, **e–h**, **j**), dorsal is up in (**c**, **d**, **i**). **a** Lateral overview, head completely retracted. Note that the lateral muscles are broken on segment 5. **b** Detail of introvert-associated muscles, head completely retracted in the trunk. **c**, **d** Cross sections at two different levels in (**b**) indicated by dashed lines and arrows. **e** Detail of mouth cone and pharynx-associated muscles. **f** Detail of cuticle of segment 1, ventral view, introvert partly extended. **f'** Close-up of dashed rectangle marked in (**f**) showing muscular scars of: dorsoventral muscle (dashed circle) and longitudinal muscles (arrows). **g** Detail of cuticle of segment 5, lateral view. Chevrons mark conspicuous muscular scars from the attachments of the longitudinal muscles of the trunk; a dashed circle marks the midlateral attachment point of the dorsoventral muscle. **h** Segments 7–11 ventral view, male. **i** Cross section at segment 9 indicated with a dashed line and arrow in (**h**). Arrows mark the position of unidentified F-actin labelling. **j** Detail of segments 9–11 from (**h**), unidentified F-actin labelling marked with a dashed circle. Arrowheads in (**b**) and (**h**) mark the attachment points of the longitudinal muscles of the trunk. Numbers refer to segments. Scale bars: 20 μm (**a–e**), 10 μm (**f–j**), 5 μm in (**f'**)

and *C. styx* six (Figs. 2a, b, 4b, d, 5a, b, 6b). The primary spinoscalids are very elongated and flexible in, *C. styx*, *F. kalenesos* and *Z. yong*, resembling tentacles or palps. However, *Z. yong* is the only species with intrinsic muscles in the primary spinoscalids (Fig. 2g). Interestingly, closely related genera like *Antygomonas*, *Tubulideres* and *Centroderes* have also been described to have intrinsic muscles, which might be a synapomorphy for kentrotrahagids (Müller and Schmidt-Rhaesa 2003; Herranz et al. 2020, Herranz pers. obs.). Other cyclorhagids, such as Echinoderidae, lack intrinsic muscles in the primary spinoscalids (Herranz et al. 2014), and no data is available for Xenosomata. Within Allomalorhagida, intrinsic muscles in the primary spinoscalids are only present in *Dracoderes* (Herranz et al. 2020).

The mouth cone is extraordinarily long in *C. styx*, *F. kalenesos* and *Z. yong* (Altenburger et al. 2015; Herranz et al. 2019; Rucci et al. 2020). The three species show circular musculature at the base of the inner and outer oral styles; however, only *Z. yong* shows small muscles associated with each of the outer oral styles, meaning that they have independent motility (Fig. 2g). Species of *Antygomonas* also have intrinsic muscles in the outer oral styles (Müller and Schmidt-Rhaesa 2003), and unpublished results also confirm their presence in other kentrotrahagids such as *Centroderes* and *Tubulideres* species (Herranz pers. obs.). This again points towards a closer relationship between *Cateria* and *Franciscideres* rather than with *Zelinkaderes*, which shows more myoanatomical similarities with other kentrotrahagids.

Neck

Among aberrant kinorhynchs, the neck is the body region that shows most morphological disparity. While *C. styx* lacks a differentiated neck, its sister species *C. gerlachi*, does have a weakly developed neck with indications of placids (Neuhaus and Kegel 2015; Herranz et al. 2019). *Triodontoderes* species have distally tripartite and differentiated placids as extensions of the first trunk segment (Sørensen and Rho 2009). *Zelinkaderes* species show a weakly defined neck with reduced placids (e.g., Higgins 1990; Dal Zotto 2013; Altenburger et al. 2015), whereas *Gracilideres* and *Franciscideres* show a cylindrical segment-like neck without placids (Dal Zotto et al. 2013; Yamasaki 2019). This morphological plasticity has an influence on the functionality of the closing apparatus and the underlying muscles. The three studied species show a radial closing apparatus. In *Z. yong* and *F. kalenesos*, the neck has associated circular musculature, showing three muscles in *Z. yong* and one single muscle in *F. kalenesos* (Figs. 2b, Fig. 4d). *C. styx* lacks a distinct neck but shows six circular muscles situated along the introvert region and anteriormost part of segment 1, which reduce the introvert diameter and assist in closing after the head is withdrawn into the trunk (Fig. 6b). *F. kalenesos* is the only species that shows longitudinal muscles in the neck. Based on their position and attachment, these muscles seem to be equivalent to the longitudinal (ventral and dorsal) muscles found in the trunk segments (Fig. 5).

Trunk

Aberrant kinorhynchs share the presence of a trunk with very thin cuticle and poorly defined segments; however, they show different segment compositions. *Cateria* species have segments 1–6 composed of a single tergal and sternal plate, and a single tergal plate with a midventral articulation on segments 7–11 (Neuhaus and Kegel 2015; Herranz et al. 2019). In *Triodontoderes* species, segment 1 is composed of one tergal and one sternal plate, segments 2–4 of one tergal and two sternal plate and segments 5–11 of one tergal plate with midventral articulation (Sørensen and Rho 2009; Cepeda et al. 2019). *Gracilideres mawatarii* Yamasaki 2019 shows all trunk segments as a closed ring (Yamasaki 2019). *F. kalenesos* has segments 1, 2 and 11 as closed cuticular rings while the remaining segments are composed of a tergal plate with weak midventral articulation (Dal Zotto et al. 2013). *Z. yong* has segments 1–2 as rings and the remaining segments as a tergal plate with a midventral articulation (Altenburger et al. 2015). Despite these differences, the underlying trunk musculature in the three studied species does not vary much. The main differences found in the trunk musculature are related to the dorsoventral and lateral muscles. Dorsoventral muscles are present

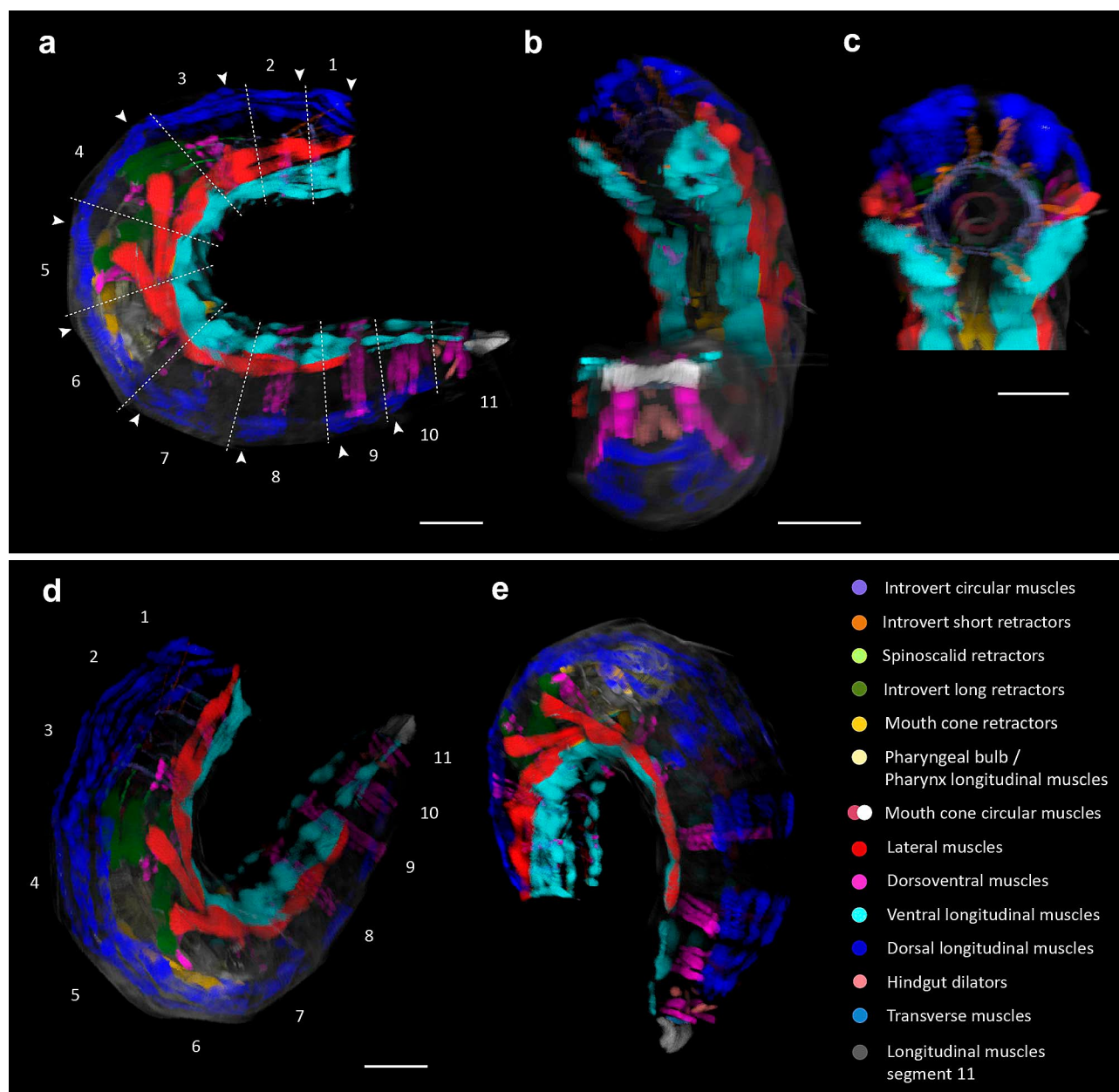


Fig. 7 Three-dimensional reconstruction of the myoanatomy in *C. styx*. Autofluorescence of the cuticle was kept for guidance in (a, b, d). Anterior is up in (b–d), right in (a) and down in (e). Colour legend applies to all panels. **a** Lateral view. Dashed lines mark segment

limits, arrowheads mark the attachment points of longitudinal muscles. **b** Ventrolateral view. **c** Detail of closing apparatus, apical view. **d, e** Laterodorsal views, right side (d), left side (e). Scale bars: 20 μm (a, b, d, e), 10 μm (c)

in all segments in *C. styx* and *F. kalenesos*, but lacking in segment 1 in *Z. yong* (Fig. 2a). These muscles have also been reported throughout the trunks of the allomalorhagid genera *Pycnophyes* and *Setaphyes* (Rothe and Schmidt-Rhaesa 2004; Schmidt-Rhaesa and Rothe 2006; Altenburger et al. 2015; Herranz et al. 2020). Some cyclorhagid genera, such as *Echinoderes*, lack dorsoventral muscles in segment 1 (Herranz et al. 2014), while in other genera such as *Antygomonas*, one species (*Antygomonas* sp.) was described as

having dorsoventral muscles in all segments (Müller and Schmidt-Rhaesa 2003). However, unpublished material of various *Antygomonas* species (Herranz pers. obs.) shows a consistent absence of dorsoventral muscles in segment 1, which would agree with the configuration found in *Z. yong*. This stresses the differences between *Z. yong* with *C. styx* and *F. kalenesos*.

The three studied species show lateral longitudinal muscles in most trunk segments (Figs. 3, 5, 7). These muscles

contribute to increase the flexibility of the trunk, especially allowing lateral movements and rotation. The position of the lateral muscles seems to be more oblique in *C. styx* and *Z. yong*, whereas it is more longitudinal—almost parallel to the ventromedial muscles—in *F. kalenesos*. Based on their position and function, the lateral muscles could be homologous with the diagonal muscles described in most cyclorhagids (Müller and Schmidt-Rhaesa 2003; Herranz et al. 2014) and *Dracoderes* (Herranz et al. 2020).

Trunk spines, excluding the terminal spines on segment 11, do not seem to be associated with muscles in any kinorhynch and are therefore assumed to move passively with the trunk (Müller and Schmidt-Rhaesa 2003; Neuhaus 2013; Herranz et al. 2014). This is confirmed also by the present study; however, we consistently found weak F-actin labelling forming a ring shape in the central part of all cuspidate spines in *Z. yong* (Fig. 2j'). The same labelling could be observed inside the cuspidate spines of *Antygomonas* species (Herranz pers. obs.), suggesting a contractile capability. The presence of a terminal pore in the distal end of all cuspidate spines is congruent with their presumed secretory function (Neuhaus 2013). Thus the F-actin ring-like labelling could correspond to a sphincter that would control the opening of the glandular pore. Based on these results, it would be expected to find similar F-actin labelling in all other genera with well-developed cuspidate spines such as *Semnoderes*, *Sphenoderes*, *Condyloderes* or *Wollunquaderes*. The terminal spines are the only trunk spines with associated musculature in the three studied species; however, there are differences in number and orientation of the muscles. In *Z. yong*, the midterminal spine is associated with two strong longitudinal muscles while in *C. styx* the midterminal spine has no musculature (Figs. 2j', 6 h). *F. kalenesos* lacks a midterminal spine but instead it has a long middorsal spine on segment 11 without associated musculature. This means that only *Z. yong* can actively move the midterminal spine and again stresses the differences from *C. styx* and *F. kalenesos*. The occurrence of muscles associated with the midterminal spine has also been described in *Antygomonas* sp. with positions identical with those described for *Z. yong* (Müller and Schmidt-Rhaesa 2003) which reflects their kentrhorhagid affinity. Unpublished studies (Herranz pers. obs.) also confirm the presence of midterminal spine muscles in *Tubulideres*. Lateral terminal accessory spines always seem to be connected with levator muscles in the three studied species. Interestingly, the lateral terminal spines do not seem to have associated musculature. But nonetheless, due to their proximity, it is possible that they can indirectly move together with the lateral accessory spines as described for *F. kalenesos*.

Functional morphology in aberrant kinorhynchs

Within Kinorhyncha, there is a great variation in cuticle thickness ranging from very robust and sclerotized plates (e.g., *Pycnophyes*, *Setaphyes*, *Dracoderes* and *Echinoderes*) to extremely thin ones as in aberrant kinorhynchs (Neuhaus 2013). The only studies including ultrastructural details of cuticle composition and thickness are from different species of *Pycnophyes*, with a cuticle of ca. 5–5.5 µm; *Echinoderes*, with ca. 3 µm; *Zelinkaderes*, ca. 1 µm and *C. styx*, ca. 0.5 µm (Moritz and Storch 1972; Kristensen and Higgins 1991; Bauer-Nebelsick 1995; Hirose and Yamasaki 2015; Herranz pers. obs.). The thickness of the cuticle also varies in the different body regions where the trunk plates, and neck placids are the thickest and most rigid, and the introvert (excluding the scalids), intersegmental and interplacid areas the thinnest and most flexible (Kristensen and Higgins 1991; Bauer-Nebelsick 1995; Neuhaus 2013). In aberrant kinorhynchs, the differences in cuticle thickness among body regions are not distinct. The cuticle is thin and flexible in most areas, except for the mouth cone, spinoscalid bases and trunk spines. In most kinorhynchs, trunk segments are articulated through soft, flexible, intersegmental cuticle and have anterior apodeme-like cuticular thickenings, named pachycycli, to which the muscles attach (Kristensen and Higgins 1991; Neuhaus 2013); however, aberrant kinorhynchs lack pachycycli (Bauer-Nebelsick 1995; Dal Zotto et al. 2013; Altenburger et al. 2015; Neuhaus and Kegel 2015; Yamasaki 2019). The absence of pachycycli affects the attachment points of the longitudinal muscles, which are posteriorly displaced into each segment leaving conspicuous markings, visible in the cuticle surface, named “muscle scars”. In the studied species, the external segmentation of the cuticle does not correlate with the segmental arrangement of the muscles, which is staggered, giving the false impression that the longitudinal muscles are continuous. The arrangement of the trunk longitudinal muscles, combined with the thin and flexible cuticle allows the trunk segments to fold. This way aberrant kinorhynchs can contract along the anterior–posterior axis further than common kinorhynchs, which have rigid segments, producing a characteristic accordion-like movement described for *C. styx* and *F. kalenesos* (Herranz et al. 2019; Rucci et al. 2020) (Online resource 1, 2). Accordion-like movements are combined with fast twisting and coiling in *C. styx* and *F. kalenesos* resembling a worm-like locomotion (Herranz et al. 2019; Rucci et al. 2020).

The neck in aberrant kinorhynchs is weakly developed, composed of very thin cuticle without well-differentiated placids, or even absent as in *C. styx* (Neuhaus and Kegel 2015; Herranz et al. 2019). Functionally, weakly developed necks do not seem to act as a closing apparatus, as

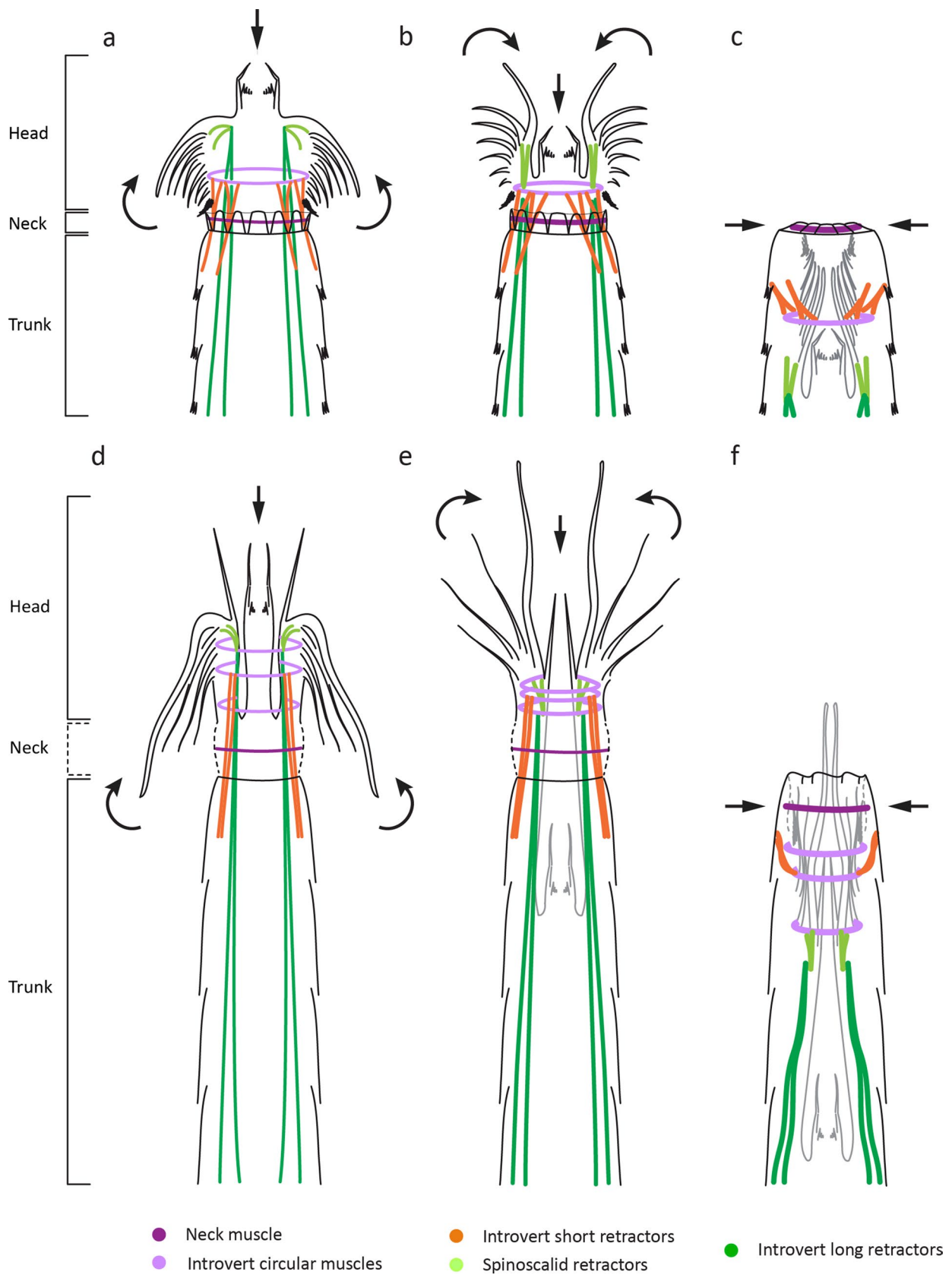


Fig. 8 Schematic showing muscle function during introvert retraction in non-aberrant (**a, b, c**, modified from Herranz et al. 2014) vs aberrant (**d–f**) kinorhynchs. Only the muscle groups considered to be directly associated with the introvert retraction are represented. Anterior is up. Arrows indicate directional movements of the introvert scalds, mouth cone and neck. Relaxed muscles are represented with thin lines while contracted muscles are represented with thick lines. The diameter of the circular muscles also represents the level of contraction. **a, d** Introvert fully everted, mouth cone protruded. **b, e** Introvert and mouth cone partially retracted. **c, f** Introvert and mouth cone fully retracted. Dashed lines in (**d–f**) represent the neck, which is lacking in some aberrant kinorhynchs (e.g., *C. styx*). Note that in (**f**) the neck is withdrawn with the introvert into the trunk while the distal end of the primary spinoscalids is left outside

they usually invert into the trunk together with the introvert (Bauer-Nebelsick 1995; Herranz et al. 2019) (Fig. 8). In *C. styx*, *F. kalenesos* and *Z. yong* the primary spinoscalids are so long that they cannot be fully withdrawn with the introvert, confirming that the neck does not act as a closing apparatus, as in most kinorhynchs, but just as an introvert constrictor (Herranz et al. 2019) (Fig. 8). In *F. kalenesos*, the neck is highly modified being unusually long. Externally it resembles an additional segment, with a slightly different cuticular ornamentation (showing parallel longitudinal furrows) when compared with trunk segments (with scale-like structures). *F. kalenesos* neck has a central circular muscle with associated longitudinal muscles that extend into segment 1. These dorsal and ventral sets of longitudinal muscles might contribute to shorten the neck length during introvert withdrawal, facilitating the scald constriction. Even though the neck in *F. kalenesos* is completely different from *C. styx* and *Z. yong*, it also lacks placids and can be withdrawn with the introvert as described in *Z. yong*. Similar to *F. kalenesos*, *G. mawatarii* shows a segment-like neck with longitudinal furrows and no placids. Due to the close relationship between *Franciscideres* and *Gracilideres* and the morphological resemblance of the neck (Sørensen et al. 2015; Yamasaki 2019), *G. mawatarii* is expected to have similar underlying muscles as *F. kalenesos*.

In all kinorhynchs, the mouth cone and introvert each possess particular musculature and neural elements, and they can move independently (Herranz et al. 2014, 2019). However, in most kinorhynchs due to their proximity, the mouth cone is indirectly moved together with the introvert during the eversion of the head and thus a full eversion of the introvert involves a protraction of the mouth cone (Fig. 8a, c). Aberrant kinorhynchs have an extraordinarily long mouth cone connected with the introvert through a long and flexible cuticle (Dal Zotto et al. 2013; Neuhaus and Kegel 2015; Herranz et al. 2019; Yamasaki 2019; Rucci et al. 2020) (Fig. 8d, f). This way, the mouth cone and introvert are physically more separated from each other (e.g., ca. 100 µm from the base of the mouth cone to the introvert spinoscalids in *C. styx*), and the introvert can be completely extended while the

mouth cone is still fully retracted into the trunk (e.g., Online resources 1–2). Live observations of *F. kalenesos* show the mouth cone being rapidly protruded and retracted independent from the introvert, confirming this interpretation (Rucci et al. 2020). We could not find mouth cone protractor muscles in *F. kalenesos* therefore, this fast movement is presumed to be produced by increased internal pressure from the fast contraction of dorsoventral muscles of the trunk. Movement of the elongated outer oral styles in *C. styx* and *F. kalenesos* is controlled by a single circular muscle that opens and closes the styles in synchrony as demonstrated by Rucci et al. (2020). Each outer oral style in *Z. yong* has, besides the circular muscles, associated longitudinal muscles which might provide additional motility.

Kinorhynch introverts are locomotory and sensorial apparatuses (Kristensen and Higgins 1991; Neuhaus 2013; Herranz et al. 2014, 2019, 2020). Locomotion in the absence of limbs is mostly carried out through the eversion, anchoring to the substrate and withdrawal of the introvert, with help of the contraction/extension of the trunk. As a result, the animal is pulled forward through the sediment (Neuhaus 2013, Herranz et al. 2014). The introvert in aberrant kinorhynchs shows multiple modifications, including the reduction in number and elongation of the spinoscalids. This is most conspicuous in the primary spinoscalids which are tentacle-like. Flexible and elongated spinoscalids as present in aberrant kinorhynchs might be less efficient for a lever-based locomotion, suggesting a more sensory and less locomotory function of the introvert. The thin and flexible cuticle of the trunk combined with the elongation and contraction of the trunk segments seem to produce the characteristic, worm-like, movement most likely responsible of the forward locomotion in aberrant kinorhynchs (see Additional files in Rucci et al. 2020).

Are aberrant kinorhynchs adapted to the interstitial environment?

It is broadly known that some of the adaptations shown by interstitial fauna are related with flexible, elongated and slender body shapes (Giere 2009). Tendencies towards vermiformity in interstitial organisms have been clearly described compared with the same organisms from different biotopes (e.g., nemerteans, nematodes, copepods, ostracods, polychaetes) (Remane 1933; Swedmark 1964; Giere 2009). Most aberrant kinorhynchs have been found associated with medium to coarse sandy sediments (Higgins 1968; Dal Zotto et al. 2013; Altenburger et al. 2015; Neuhaus and Kegel 2015; Herranz et al. 2019; Lopes Mello et al. 2019; Rucci et al. 2020; Yamasaki 2019) with some exceptions such as *Zelinkaderes floridensis* Higgins, 1990, that is found in mud (Higgins 1990). The length-to-width ratio in aberrant kinorhynchs is at least twice as much as in other kinorhynchs.

C. styx, *Z. yong*, *F. kalenosos* and *G. mawatarii* show ratios above 10:1 compared with e.g.,: *Pycnophyes*, *Paracentrophyes*, *Dracoderes* and *Condyloderes* ranging from 3–4:1; *Echinoderes*, 4–5:1 and *Tubulideres*, *Sphenoderes* 6:1 (data obtained from Sørensen et al. 2012; Dal Zotto et al. 2013; Neuhaus and Kegel 2015; Sørensen and Landers 2017; Herranz et al. 2018, 2019; Rucci et al. 2020; and others). These ratios are approximate due to the variability in the level of contraction or extension of the trunk but still show a clear difference in the proportions between aberrant and common kinorhynchs. The combination of a slender, vermiform body and a flexible cuticle should be regarded an adaptation to life in interstitial habitats (Giere 2009; Yamasaki 2019). The current phylogenetic positions of worm-like kinorhynchs, nested in distantly related clades of the tree (see Sørensen et al. 2015), suggest that their characteristic vermiform appearance evolved convergently, most likely driven by an ecological shift in niches from muddy sediments to sandy interstitial environments. However, it is important to stress that not all interstitial kinorhynchs show elongated trunks and thin cuticle, which is the case for several species of interstitial *Echinoderes* and *Cephalorhyncha* (see Higgins 1986; Sørensen 2008; Sánchez et al. 2012; Yildiz et al. 2016).

Conclusions

This study shows that a body plan with segmentally arranged musculature remains conserved across Kinorhyncha, both morphologically and functionally. Despite their vermiform appearance, aberrant kinorhynchs have segmentally arranged musculature. However, differing from most kinorhynchs, where longitudinal muscles attach to the pachycycli situated at the anterior segment margins, the muscles of aberrant kinorhynchs attach more posteriorly. The attachment points for the longitudinal muscles in the trunk of aberrant kinorhynchs are instead displaced to the anteriormost part, or the central part, of each tegumental plate. The lack of pachycycli is associated with the extremely thin and flexible cuticle characteristic of the worm-like kinorhynchs.

Morphologically and myoanatomically, *C. styx* shows more resemblance with *F. kalenosos*, than it does with *Z. yong*. This suggests that *Cateria* is more closely related to allomalorhagids than to cyclorhagids. The distant phylogenetic positions of *Zelinkaderes* and *Franciscideres* (and possibly *Cateria*) suggest that the aberrant appearance evolved at least twice independently, and that it most likely reflects an adaptation to the interstitial environment.

Supplementary Information The online version contains supplementary material available at <https://doi.org/10.1007/s00435-021-00519-3>.

Acknowledgments We are grateful to the Bioimaging facility of University of British Columbia, to the Unidade Integrada de Imagens e Laboratório de Invertebrados from Instituto de Biodiversidade e Sustentabilidade, Federal University of Rio de Janeiro UFRJ (NUPEM/UFRJ—Macaé) for offering laboratory space; and to Center for Marine Studies, Federal University of Paraná (CEM/UFPR) for offering lab space and student support with field collections in Pontal du Sul in 2015 and 2019.

Author contribution MH, MVS, KW conceived the study. MH, MVS, KW, TP, and MDD collected specimens from South Korea and Brazil. MH prepared and performed the experiments and imaging at the University of Copenhagen and University of British Columbia. MH prepared all figures and 3D reconstructions. MH, MVS, and KW drafted the manuscript. All authors have proofed and approved the final version of this manuscript.

Funding This project received funding from the European Union's Horizon 2020 research and innovation programme, under the Marie Skłodowska-Curie grant agreement No 797140 to MH. Sampling in South Korea was funded by the Carlsberg Foundation to MVS (CF17-0054). CLSM facilities were supported by the Villum foundation (Grant # 102544) and the Carlsberg Foundation to KW (CF15-0946). CLSM imaging at the University of British Columbia was funded by the Hakai Institute (Tula foundation) and the National Science and Engineering Research Council of Canada (NSERC 2019–03986) to BSL.

Data availability All data analysed during this study is included in the present contribution and its associated files (online resources 1 and 2).

Compliance with ethical standards

Conflict of interest The authors declare that they do not have any conflict of interest.

References

- Altenburger A (2016) The neuromuscular system of *Pycnophyes kielensis* (Kinorhyncha: Allomalorhagida) investigated by confocal laser scanning microscopy. *EvoDevo* 7(1):25. <https://doi.org/10.1186/s13227-016-0062-6>
- Altenburger A, Rho HS, Chang CY, Sørensen MV (2015) *Zelinkaderes yong* sp. nov. from Korea—the first recording of *Zelinkaderes* (Kinorhyncha: Cyclorhagida) in Asia. *Zool Stud* 54:25. <https://doi.org/10.1186/s40555-014-0103-6>
- Bauer-Nebelsick M (1995) *Zelinkaderes klepali* sp. n., from shallow water sands of the Red Sea. *Ann Nat Mus Wien* 97B:57–74
- Cepeda D, Sánchez N, Pardos F (2019) First report of the family Zelinkaderidae (Kinorhyncha: Cyclorhagida) for the Caribbean Sea, with the description of a new species of *Triodontoderes* Sørensen and Rho, 2009 and an identification key for the family. *Zool Anz* 282:116–126. <https://doi.org/10.1016/j.jcz.2019.05.017>
- Dal Zotto M, Di Domenico M, Garraffoni A, Sørensen MV (2013) *Franciscideres* gen. nov.—a new, highly aberrant kinorhynch genus from Brazil, with an analysis of its phylogenetic position. *Syst Biodivers* 11:303–321. <https://doi.org/10.1080/14772000.2013.819045>
- Gerlach SA (1956) Über einen aberranten Vertreter der Kinorhynchen aus dem Küstengrundwasser. *Kieler Meeresforsch* 12:120–124
- Giere O (2009) *Meiobenthology. The microscopic motile fauna of aquatic sediments*, 2nd edn. Springer, Berlin, p 527

- Herranz M, Pardos F, Boyle MJ (2013) Comparative morphology of serotonergic-like immunoreactive elements in the central nervous system of kinorhynchs (Kinorhyncha, Cyclorhagida). *J Morphol* 274:258–274. <https://doi.org/10.1002/jmor.20089>
- Herranz M, Boyle MJ, Pardos F, Neves RC (2014) Comparative myoanatomy of *Echinoderes* (Kinorhyncha): a comprehensive investigation by CLSM and 3D reconstruction. *Front Zool* 11:1–26. <https://doi.org/10.1186/1742-9994-11-31>
- Herranz M, Yangel E, Leander BS (2018) *Echinoderes hakaiensis* sp. nov.: a new mud dragon (Kinorhyncha, Echinoderidae) from the northeastern Pacific Ocean with the redescription of *Echinoderes pennaki* Higgins, 1960. *Mar Biodiv* 48:303–325. <https://doi.org/10.1007/s12526-017-0726-z>
- Herranz M, Di Domenico M, Sørensen MV, Leander BS (2019) The enigmatic kinorhynch *C. styx* Gerlach, 1956—a sticky son of a beach. *Zool Anz* 282:10–30. <https://doi.org/10.1016/j.jcz.2019.05.016>
- Herranz M, Sørensen MV, Park T, Leander BS, Worsaae K (2020) Insights into mud dragon morphology (Kinorhyncha, Allomalorhagida): myoanatomy and neuroanatomy of *Dracoderes abei* and *Pycnophyes ilyocryptus*. *Org Divers Evol* 20:467–493. <https://doi.org/10.1007/s13127-020-00451-2>
- Higgins RP (1968) Taxonomy and postembryonic development of the Cryptorhagae, a new suborder for the mesopsammic kinorhynch genus *Cateria*. *Trans Amer Microsc Soc* 87:21–39
- Higgins RP (1986) A new species of *Echinoderes* (Kinorhyncha: Cyclorhagida) from a coarse-sand California beach. *Trans Am Microsc Soc* 105:266–273
- Higgins RP (1990) *Zelinkaderidae*, a new family of cyclorhagid Kinorhyncha. *Smithson Contr Zool* 500:1–26
- Hirose E, Yamasaki H (2015) Fine structure of the integumentary cuticles and alimentary tissues of pycnophyid kinorhynchs *Pycnophyes oshoroensis* and *Kinorhynchus yushini* (Kinorhyncha, Homalorhagida). *Zool Sci* 32:389–395. <https://doi.org/10.2108/zs150021>
- Kristensen RM, Higgins RP (1991) Kinorhyncha. In: Harrison FW, Ruppert EE (eds) *Microscopic anatomy of invertebrates, The Aschelminthes*, vol 4. Wiley, New York, pp 377–404
- Lopes Mello C, Carvalho AL, Cabral de Faria L, Baldoni L, Di Domenico M (2019) Spatial distribution pattern of the aberrant *Franciscideres kalenesos* (Kinorhyncha) on sandy beaches of Southern Brazil. *Zool Anz* 282:44–51. <https://doi.org/10.1016/j.jcz.2019.05.008>
- Moritz K, Storch V (1972) Zur Feinstruktur des Integumentes von *Trachydemus giganteus* (Kinorhyncha). *Z Morphol Tiere* 71:189–202
- Müller MCM, Schmidt-Rhaesa A (2003) Reconstruction of the muscle system in *Antygomonas* sp. (Kinorhyncha, Cyclorhagida) by means of phalloidin labeling and cLSM. *J Morphol* 256:103–110. <https://doi.org/10.1002/jmor.10058>
- Nebelsick, (1993) Introvert, mouth cone, and nervous system of *Echinoderes capitatus* (Kinorhyncha, Cyclorhagida) and implications for the phylogenetic relationships of Kinorhyncha. *Zoomorphology* 113:211–232. <https://doi.org/10.1007/BF00403313>
- Neuhaus B (1994) Ultrastructure of alimentary canal and body cavity, ground pattern, and phylogenetic relationships of the Kinorhyncha. *Microfauna Mar* 9:61–156
- Neuhaus B (2013) Kinorhyncha (=Echinodera). In: Schmidt-Rhaesa A (ed) *Handbook of Zoology. Gastrotricha, Cycloneuralia and Gnathifera. Volume 1: Nematomorpha, Priapulida, Kinorhyncha, Loricifera*. De Gruyter, Berlin/Boston, pp. 181–348
- Neuhaus B, Kegel A (2015) Redescription of *Cateria gerlachi* (Kinorhyncha, Cyclorhagida) from Sri Lanka and of *C. styx* from Brazil, with notes on *C. gerlachi* from India and *C. styx* from Chile, and the ground pattern of the genus. *Zootaxa* 3965:1–77. <https://doi.org/10.11646/zootaxa.3965.1.1>
- Remane A (1933) Verteilung und Organisation der benthonischen Mikrofauna der Kieler Bucht. *Wiss Meeresuntersuch* 21:161–221
- Rothe B, Schmidt-Rhaesa A (2004) Probable development from continuous to segmental longitudinal musculature in *Pycnophyes kielenensis* (Kinorhyncha Homalorhagida). *Meiofauna Marina* 13:21–28
- Rucci KA, Neuhaus B, Bulnes VN, Cazzaniga NJ (2020) New record of the soft-bodied genus *Franciscideres* (Kinorhyncha) from Argentina, with notes on its movement and morphological variation. *Zootaxa* 4780:107–131. <https://doi.org/10.11646/zootaxa.4780.1.5>
- Sánchez N, Herranz M, Benito J, Pardos F (2012) Kinorhyncha from the Iberian Peninsula: new data from the first intensive sampling campaigns. *Zootaxa* 3402:24–44. <https://doi.org/10.11646/zootaxa.3402.1.2>
- Schmidt-Rhaesa A, Rothe B (2006) Postembryonic development of dorsoventral and longitudinal musculature in *Pycnophyes kielenensis* (Kinorhyncha, Homalorhagida). *Integr Comp Biol* 46:144–150. <https://doi.org/10.1093/icb/icj019>
- Sørensen MV (2008) A new kinorhynch genus from the Antarctic deep-sea and a new species of *Cephalorhyncha* from Hawaii (Kinorhyncha: Cyclorhagida: Echinoderidae). *Org Div Evol* 8:233–246. <https://doi.org/10.1016/j.ode.2007.11.003>
- Sørensen MV, Landers SC (2017) Description of a new species, *Paracentrophyes sanchezae* n. sp. (Kinorhyncha: Allomalorhagida) from the Gulf of Mexico, with differential notes on one additional, yet undescribed species of the genus. *Zootaxa* 4242:61–76. <https://doi.org/10.11646/zootaxa.4242.1.3>
- Sørensen MV, Pardos F (2020) Kinorhyncha. In: Schmidt-Rhaesa A (ed) *Guide to the identification of Marine Meiofauna*. Verlag Dr Friedrich Pfeil, Munich, pp 391–414
- Sørensen MV, Rho HS (2009) *Triodontoderes anulap* gen. et sp. nov.—a new cyclorhagid kinorhynch genus and species from Micronesia. *J Mar Biol Assoc UK* 89:1269–1279. <https://doi.org/10.1017/S0025315409000526>
- Sørensen MV, Heiner I, Ziemer O, Neuhaus B (2007) *Tubulideres seminoli* gen. et sp. nov. and *Zelinkaderes brightae* sp. nov. (Kinorhyncha, Cyclorhagida) from Florida. *Helgoland Mar Res* 61:247–265
- Sørensen MV, Herranz M, Rho HS, Min W, Yamasaki H, Sánchez N, Pardos F (2012) On the genus *Dracoderes* Higgins & Shirayama, 1990 (Kinorhyncha: Cyclorhagida) with a redescription of its type species, *D. abei*, and a description of a new species from Spain. *Mar Biol Res* 8:210–232. <https://doi.org/10.1080/17451000.2011.615328>
- Sørensen MV, Dal Zotto M, Rho HS, Herranz M, Sánchez N, Pardos F, Yamasaki H (2015) Phylogeny of Kinorhyncha based on morphology and two molecular loci. *PLoS ONE* 10(7):e0133440. <https://doi.org/10.1371/journal.pone.0133440>
- Swedmark B (1964) The interstitial fauna of marine sand. *Biol Rev* 39:1–42
- Yamasaki H (2019) *Gracilideres mawatarii*, a new genus and species of Franciscideridae (Allomalorhagida: Kinorhyncha)—a kinorhynch with thin body cuticle, adapted to the interstitial environment. *Zool Anz* 282:176–188. <https://doi.org/10.1016/j.jcz.2019.05.010>
- Yamasaki H, Hiruta SF, Kajihara H (2013) Molecular phylogeny of kinorhynchs. *Mol Phylogenet Evolut* 67:303–310. <https://doi.org/10.1016/j.ympev.2013.02.016>
- Yildiz NÖ, Sørensen MV, Karaytuğ S (2016) A new species of *Cephalorhyncha* Adrianov, 1999 (Kinorhyncha: Cyclorhagida) from the Aegean Coast of Turkey. *Helgol Mar Res* 70:24. <https://doi.org/10.1186/s10152-016-0476-5>